Ag/Al2/O3 ethylene epoxidation catalysts
tracking the active phase evolution

van de Poll, R.C.J.

Award date:
2018

Technische Universiteit
Eindhoven
University of Technology

Where innovation starts

Ag/Al_2O_3 ethylene epoxidation catalysts: tracking the active phase evolution

Rim C.J. van de Poll
Student ID: 0858622
r.c.j.v.d.poll@student.tue.nl

Supervisors:
Ir. A.J.F. van Hoof
Prof. dr. ir. E.J.M. Hensen
Dr. H. Friedrich

Committee:
Dr. N. Kosinov

Department of Chemical Engineering
Inorganic Materials Chemistry
Eindhoven University of Technology

Eindhoven, The Netherlands, 6th July 2018

Abstract

The influence of both oxygen coverage on the selectivity of an Ag/Al_2O_3 catalyst and the influence of industrial reaction conditions on the structure of individual nanoparticles was investigated. By pulsing ethylene over a pre-oxidized catalyst we were able to slowly remove oxygen from the silver surface. With decreasing oxygen coverage the selectivity also decreased. Performing TPD at selected points confirmed the decrease of oxygen with an increasing amount of dosed ethylene. TPD profiles were fitted to give an estimate for ratio of different oxygen types present.

It can be concluded that with decreasing oxygen coverage selectivity goes down. There also was a shift in the composition of different oxygen species during the drop in selectivity. This means that the nature of the oxygen species also has an influence on selectivity. Copper promotion yielded similar results with copper possibly changing the surface stability to the extent of influencing the ratio between different oxygen species.

Silver supported catalysts were deposited on silicon nitride wafers and were indexed using SEM and TEM. Reaction under industrial conditions (225 °C and 20 bar) were carried out on the wafers after which TEM images were taken of the same areas. Particle size analysis and event analysis was carried out on each individual area. This data was combined and an analysis was made for two reactions of 60 hours. Pore formation was found to affects around 1-10% of all large particles during 120 h of reaction. Pore formation seems to be unaffected by chlorine addition or cesium promotion. No pore formation was observed for small particles, which is likely due to the fact that small particles do not have the grain boundaries or amount of subsurface oxygen to facilitate pore growth.

The combination of cesium promotion and chlorine moderation seemed to stabilize the particle growth on the catalyst, which could be connected to improved catalytic performance of the cesium promoted catalysts. A process of particle wetting was observed for large and cesium promoted particles. This process affects a large part of particles (15%) which makes it one of the major particle growth mechanisms for the silver system. The exact nature on how it affects the

Contents

Introduction

Energy is one of the most important issues in all of human history. In prehistoric times fire could keep you warm and allowed you to cook food. In antiquity the energy from human muscle power allowed man to create the pyramids and other great wonders of the world. At the end of the middle ages the energy in gunpowder allowed the Europeans to expand their empires and conquer vast stretches of the world. With the dawn of the 18th century man discovered the steam engine and with that was able to release vast amounts of energy long stored in the earth's crust in the form of coal. In the 20th century the Second World War showed that the control of oil, and with that energy, was vital for a country's survival.

Each of these energy sources had their own challenges associated with them. And now in the 21st century another great energy challenge is presented. How can we, as humans, produce enough energy to meet our energy demands without destroying our planet in the process? This is where catalysis may play an important role. While catalysts generally cannot be used for the production of energy themselves, they can be used to make it more efficient or reduce emissions from the processes that produce the energy. An example of this would be the three-way catalyst in a car's exhaust. The engine burns fuel, but in doing so, produces carbon monoxide, NO_x and CH_x. A catalyst is then used to convert these gases to less harmful substances. In the end the car's engine can produce the energy needed for driving while the catalyst mitigates the damage of the gases produced.

What is catalysis?

A catalyst is a substance which can enhance the rate of a chemical reaction and facilitate this at milder conditions. The overall reaction barrier is lowered but the thermodynamic start and end states remain unchanged. In Figure 1 a systematic overview of the catalytic Haber-Bosch reaction can be seen. In this reaction hydrogen (blue) and nitrogen (green) are combined to form ammonia. The first step involves the adsorption and subsequent dissociation of hydrogen and nitrogen on the surface of the catalyst. In the next step hydrogen atoms are attached one by one to the nitrogen atom in three elementary reaction steps forming ammonia (NH_3). In the final step ammonia desorbs from the surface into the gas phase and can be transported away. In the end the reaction products are the same, but the activation energy ($E_{a,\,cat}$ in figure) is lowered.

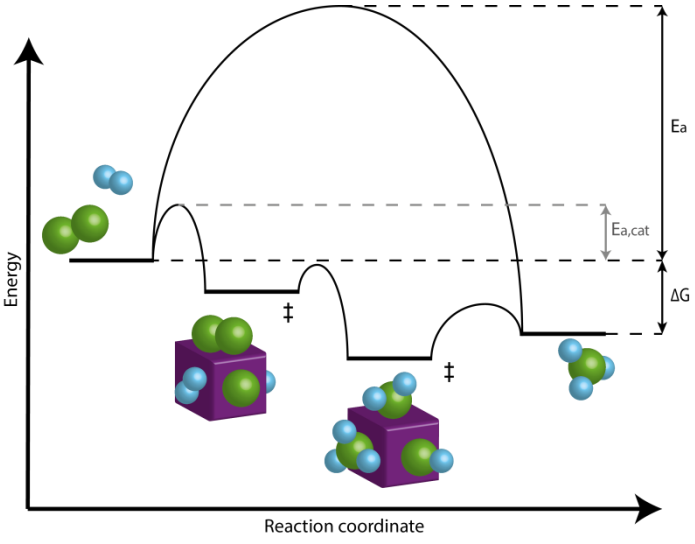

Figure 1. A schematic overview of the catalytic Haber-Bosch reaction. Blue = hydrogen, Green = Nitrogen.

Depending on the nature of catalysts the catalytic processes are generally divided into three groups: heterogeneous, homogeneous and biocatalysis.

In heterogeneous catalysis the catalyst and reactant are present in different phases. In industry the majority of heterogeneous catalysts are present in the solid state, with the reactants being present in the liquid or gaseous state. A big advantage of solid catalysts is that it can be immobilized in the reactor, removing the need to carry out costly separation steps. An example of heterogeneous catalysts is the Haber-Bosch process. In this process hydrogen and nitrogen gas are converted into ammonia by flowing gases over a metal catalyst, most commonly iron.

In homogeneous catalysis the catalyst and reactants are both present in the same phase, usually liquid. Homogeneous catalysts find their main application in pharmaceutical and fine chemical industries. One of the advantages of homogeneous catalysts in these industries is the higher selectivities and possibility for stereo selectivity which heterogeneous catalysts can rarely provide. A disadvantage is the higher costs associated with both production and separation of homogeneous catalysts. Generally homogeneous catalysts are more expensive than heterogeneous catalysts due to their more complex nature, especially synthesis of ligands can be quite costly. Also homogeneous catalysts require an additional step to separate them from the reaction products contributing to higher total processing cost. However since pharmaceutical and fine chemical industries have more valuable products the use of a more costly catalyst can be justified. An example of homogeneous catalysis is a Friedel-Crafts alkylation of benzene with an anhydrous aluminium trichloride.

Biocatalysts are a special group of homogeneous catalysts that can be found in nature. The structure and composition of these catalysts have evolved over millions of years to obtain their current form and function and are of vital importance for life as we know it. Every living being uses biocatalysts for its metabolism and to create the building blocks for life. Biocatalysts consist of multiple amino acids that are bound together and arranged in 3D structures. A major advantage of biocatalysts is that they have very high selectivity and also sometimes stereo selectivity. One disadvantage is that they are very sensitive to operating conditions such as temperature, pollutants, pH or pressure, which have to be very mild. An example from the human body is the enzyme Amylase. This enzyme is present in our mouth and is used to catalyze the hydrolysis of starch into sugars. Typical examples of use in industry are the production of bread or beer using yeast.

Usage of ethylene oxide

Ethylene oxide is an intermediate bulk chemical with an annual world production of 34.5 million tons in 2016 [1], [2]. However due to its reactivity EO is usually converted to other products and not used directly. One of the main products is ethylene glycol (EG) of which the reaction can be seen in equation 1.

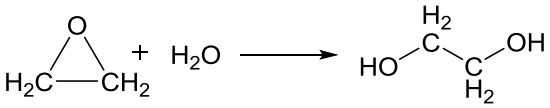

1

Two of the main uses of EG are that it can be used as antifreeze in among others the radiators of cars. The other main use lies in the production of polyesters of which polyethylene terephthalate (PET) is probably the best known.

In Shell's OMEGA process the process to create EG is combined with the production of EO to reach selectivities of 99.5% [3]. In this process EO reacts with CO_2 to create ethylene carbonate which can react with water to EG and release CO_2, which is recycled back into the process. The reaction scheme of this reaction can be seen in equation 2.

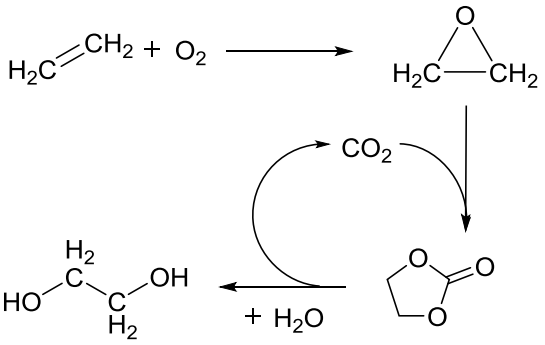

2

One of the applications were ethylene oxide can be used directly is as a disinfectant. As EO penetrates through the pores of packaging and clothing it can be used in the sterilization of hospital equipment. In this process one does have to consider the safety aspects as EO is very toxic, flammable and carcinogenic. Therefore nowadays its sterilization applications are limited to only specialized tasks.

History

Silver is one of the oldest metals known to man with its discovery predating any written records. The oldest findings of silver that can be dated accurately, can be found in Egypt in around 4000 B.C.[4]. The silver from these findings was probably purified by cupellation, a technique still used today. During cupellation ores containing multiple metals are heated to very high temperatures. Base metals will then oxidize or react with other components and form slag which then can be separated from the noble metals.

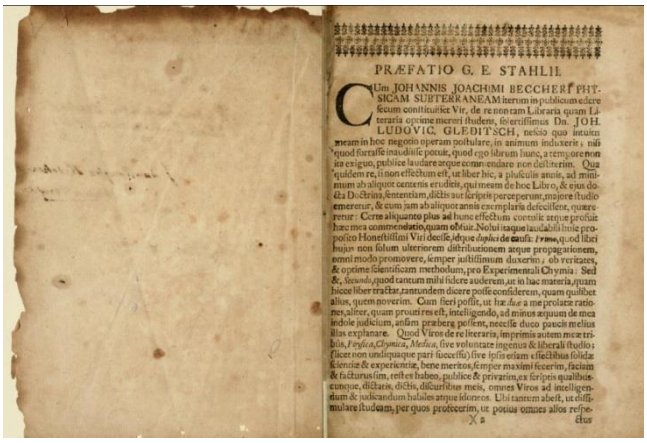
PRÆFATIO G. E. STAHLII.

CUm JOHANNIS JOACHIMI BECCHERI PHYSICAM SUBTERRANEAM iterum in publicum edere secum constituisset Vir, de re non tam Libraria quam Literaria optime merenti studens, fo: ertissimus Dn. JOH. LUDOVIC. GLEDITSCH, nexio quo inter meam in hoc negotio operam postulare, in animum induxerit, nihil quod fortasse inaudisse potuit, quod ego librum hunc, a tempore non ita exiguo, publice laudare atque commendare non desiterim. Qua equidem re, li non effectum est, ut liber hic, a plusculis annis, ad minimum ab aliquot centenis eruditis, quinnem de hoc Libro, & eius doctrina Doctrina, sententiam, dictis aut scriptis perceperunt, majore studio emeretur, & cum jam ab aliquot annis exemplaria deficiens, quærerentur: Certe aliquanto plus ad hunc effectum conferre atque profuit hæc mea commendatio, quam obtair. Nobui itaque laudabili huic propositio Honestissimi Viri deesse, idque duplici de causa: primo, quod libri hujus non solum ulteriorem distributionem atque propagationem, omni modo promovere, semper justissimum duxerim; ob veritates, & optimæ scientiæ methodum, pro Experimentali Chymia: Sed &, Secundo, quod tantum mihi fidere auderem, ut in hac materia, quam hicce liber tractat, tantundem dicere posse confiderem, quam quilibet alius, quem noverim. Cum fieri possit, ut hæ fue a me prolatæ rationes, aliter, quam prout res est, intelligendo, ad minus æquum de mea indole judicium, anfam præbere possent, necesse duco paucis melius illas explanare. Quod Viros de re literaria, imprimis autem meæ tribus, Physica, Chymica, Medica, sive voluntate ingenua & liberali studio; sicer non undiquaque pari successu) sive ipsis etiam effectibus solidæ scientiæ & experientiæ, bene meritos, semper maximi fecerim, faciam & facturus sim, res est habeo, publice & privatim, ex scriptis qualibuscunque, dictaris, dictis, discursibus meis, omnes Viros ad intelligendum & judicandum balsles atque idoneos. Ubi tantum abeit, ut dissimulare studeam, per quos profecerim, ut potius omnes alios refpe-

Figure 2. First page of Physica Subterranea written by Johann Joachim Becher in 1669. Note all texts are in Latin.

The discovery of ethylene can be traced back to 1669 by Johann Joachim Becher who published his findings in the book Physica Subterranea[5]. He described the production of a gas by heating ethanol in the presence of sulfuric acid. More interesting however, is that the ancient Egyptians had also already discovered ethylene, without even knowing about it. Namely, in order to ripen figs Egyptians placed them in a room and gash the figs to make them ripen faster[6]. What is known today is that in this process figs release ethylene which acts as a plant hormone and stimulates ripening. Now imagine if at the time an ancient Egyptian metal smelter had some figs ripening in his workshop, while he was in the process of smelting some silver. He could have been the first person to oxidize ethylene to ethylene oxide using a silver catalyst without even knowing it. However, understanding of this process would have to wait about six millennia.

The original process for the production of ethylene oxide was discovered in 1859 by Charles-Adolphe Wurtz. This used chlorohydrin combined with potassium hydroxide to produce EO and calcium chloride, see reaction equation 3 and 4. One major disadvantage of this earlier route was the chlorine compounds it produced. This however did not stop industry as BASF started the manufacture of EO using the chlorohydrin route in 1914 [7].

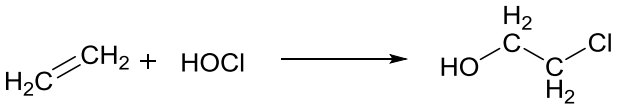

3

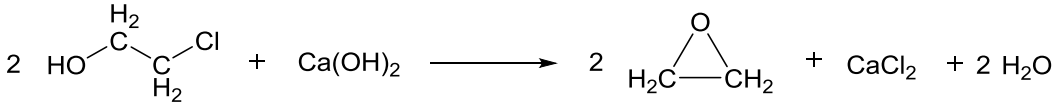

4

In 1931 Theodore Lefort made a crucial discovery, namely that metallic silver could be used as a catalyst for the direct oxidation of ethylene with oxygen, reducing the need for chlorine components. Industry quickly adapted and in 1935 Union Carbide started development on this new method of epoxidation. Two years later Union Carbide would start up their new process at their plant in South Charleston[8][9]. At the time an unpromoted silver catalyst was used which had a selectivity of 50%[7].

Silver

Why silver for epoxidation?

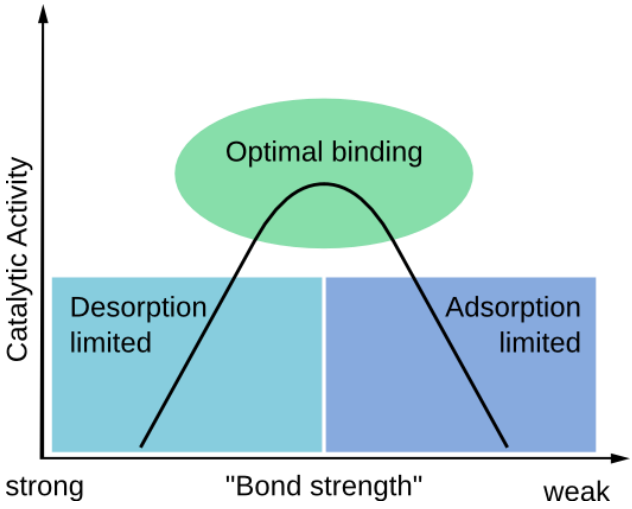

Figure 3. Systematic indication of Sabatier's principle.

For the direct epoxidation reaction of ethylene to ethylene oxide, silver is almost exclusively used as there are no other metals known that can yield comparable selectivity. Elements like copper or gold, which are above and below silver in the periodic table, are known to have activity for other oxidation reactions [10]. However the reason that silver works best for EO epoxidation is best explained through Sabatier's principle. This states that there exists an optimum for the binding between reactants and a catalyst. If the reactants bind to strong with the catalyst, they can easily absorb and react, but the formed products cannot desorb easily and the reaction is limited. On the other hand if the reactants do not bind strongly enough, no species get adsorbed and no reaction can take place.

In the case of ethylene epoxidation the critical reactant is oxygen. If oxygen is adsorbed too strongly to the metal surface, the reaction barrier for the reaction to ethylene oxide becomes too high and the reaction slows down. If the oxygen does not adsorb strong enough no oxygen will be present on the metal surface. The theoretical work done by Özbek *et al.*[11][12] on silver, copper and gold will be used to illustrates this point. The authors compared the reaction barriers of silver, copper and gold oxides for the epoxidation reaction. Copper was shown to oxidize easily, but the subsequent reaction with ethylene was difficult. Gold oxides were found to be unstable and can be compared to a situation where oxygen binding is too weak. The energy barriers of reactions with silver were found to lie between those of copper and gold, making silver the more suitable catalyst for ethylene epoxidation.

Reaction mechanism

The epoxidation of ethylene is a typical example of a catalytic process, because the product that is thermodynamically favored, is not favored in the catalytic reaction. An indirect proof of this is that at the moment the highest reported industrial selectivity is 92% towards ethylene oxide[13], which can only be achieved if the process is kinetically limited. In equation 5 it can be seen that k1 is the selective pathway in which ethylene reacts with oxygen in the presence of silver. K2 shows the unselective pathway towards acetaldehyde, which is easily converted to CO_2 and water in the presence of silver, k4. The last pathway, k3, is the isomerization of ethylene oxide to acetaldehyde. In literature is has been shown that this reaction requires a strong acid group to be present [14]. This acid group can usually be found on various supports. This is one of the reasons why EO epoxidation catalysts prefer the use of ultrapure low surface area α-alumina, free of acid hydroxyls [7].

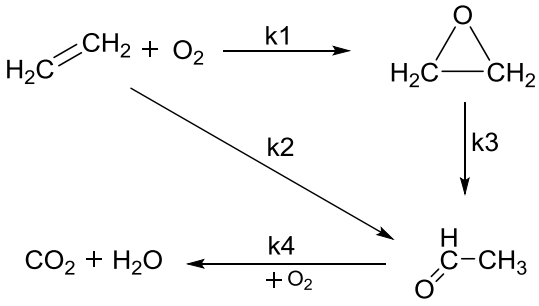

5

Oxygen

The exact mechanism of ethylene epoxidation is still debated in literature today. One of the critical points is the nature of the oxygen species. In literature multiple oxygen species are proposed and investigated, ranging from nucleophilic and electrophilic to subsurface, molecular and atomic oxygen. In this section these different oxygen theories and definitions will be discussed.

One of the earlier models for absorbed oxygen is the molecular and atomic model reported by Voge [15] in 1968. He proposed that oxygen can adsorb in its molecular form and that only the molecular form is reactive towards ethylene oxide. The remaining atomic oxygen would react towards CO_2 and water (equation 6 and 7). It can be seen that in equation 6, the selective reaction to EO produces one atomic oxygen which needs to be converted to the unselective product in equation 7. Based on this mechanism a theoretical maximum possible selectivity of 6/7 or 85.7% can be reached, which for a long time was considered to be the limit. However nowadays an industrial selectivity of 92% [13] has been reported, meaning that this mechanism could not be true in this form.

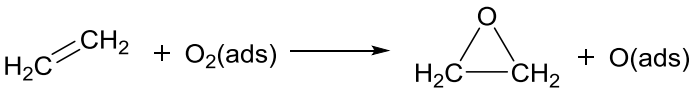

6

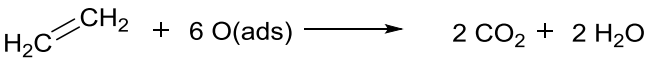

7

A variation on this atomic and molecular model is based on a classical Eley-Rideal mechanism with multiple authors reporting such mechanisms [9][16][17]. In these models oxygen adsorbs onto the surface and ethylene reacts from the gas phase with the surfaces oxides to form ethylene oxide which, depending on the model, is first adsorbed on the surface or immediately released to the gas phase.

A term that is often used in literature with regards to ethylene epoxidation on silver is subsurface oxygen. It is possible for oxygen to adsorb onto the surface of a silver particle. Based on the most common oxidation state of silver (being +1), this surface would consist of Ag_2O. However in literature authors found that a second kind of oxygen was present in silver systems, namely subsurface oxygen. This oxygen is present under the surface inside the silver particle. The exact nature and bonds this oxygen makes are still debated, ranging from just under the initial Ag_2O layer to deep in the bulk of the particle. Multiple source report that this subsurface oxygen is needed for the formation of EO [18][19][20][21]. Some examples from literature of the reactivity and behavior of this oxygen will be discussed next.

Backx *et al.* [22] were able to show that on a Ag(110) single crystal there exists a subsurface reservoir that can exchange its oxygen content with the atmosphere above. From this behavior they concluded that the subsurface oxygen would have to be close in the lattice near the surface. In experiments from Campbell et al.[23], oxygen was titrated from the surface by reaction with CO. The authors were able to show that there are at least two different types of oxygen present on a single crystal. The first being a reactive form that can react immediately upon contact with CO. The second being some form of subsurface oxygen that requires heating in order to become reactive. Under the vacuum conditions that Campbell *et al.*[23] used, they found that the suspected subsurface oxygen could be brought out of the bulk to the surface at 470 K and further desorption was found to occur at 600 K. Van Santen and de Groot [24] later showed that labeled subsurface oxygen can end up in EO, and more importantly, that subsurface oxygen needs to be present in order for EO to form.

Generally nucleophilic and electrophilic oxygen species can be distinguished. Schlögl et al. [25][26], were able to link two different oxygen species on the surface of silver to the selectivity of the reaction. The authors identified these species as nucleophilic and electrophilic oxygen, with electrophilic being the more selective species. This experimental evidence supports the earlier hypothesis of Van Santen *et al.* [27] as seen in Figure 4. Van Santen *et al.* [27] proposed that the electrophilic oxygen would attack the double bond of ethylene, whereas nucleophilic oxygen would attack the C-H bond. Electrophilic oxygen would be stabilized by the presences of subsurface oxygen, Figure 4a, possibly explaining reports of the need for subsurface oxygen for selective epoxidation.

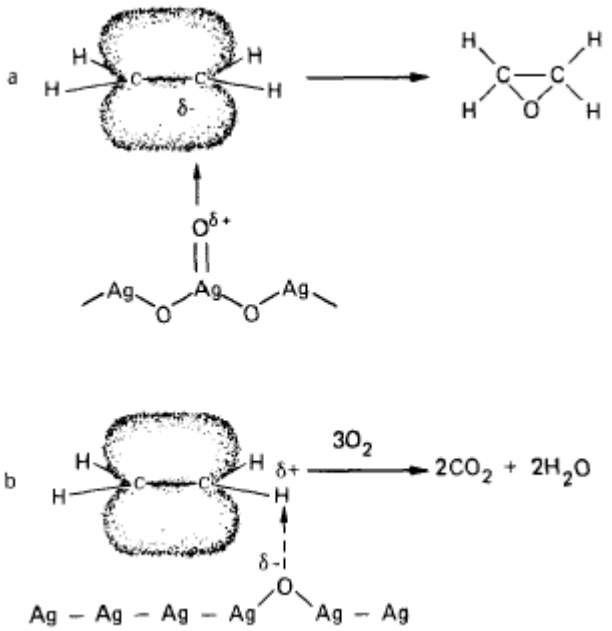

Figure 4. Schematic representation of the effect of electrophilic and nucleophilic oxygen. Taken from Van Santen *et al.* [27].

Oxometallacycle mechanism

In contrast to the previous mechanism, the oxometallacycle (OMC) mechanism uses a common C_2H_5O species. This OMC species can react to both EO and acetaldehyde (AA), where AA reacts further to CO_2 and water. In this mechanism the selectivity depends mainly on the reaction barriers of k1 and k2, see Figure 5. One of the main differences with this model is that both the reaction to EO and AA proceed through the same oxygen bearing specie, the OMC. In this mechanism the state of oxygen reacting with ethylene should not have an impact on the eventual selectivity of the reaction.

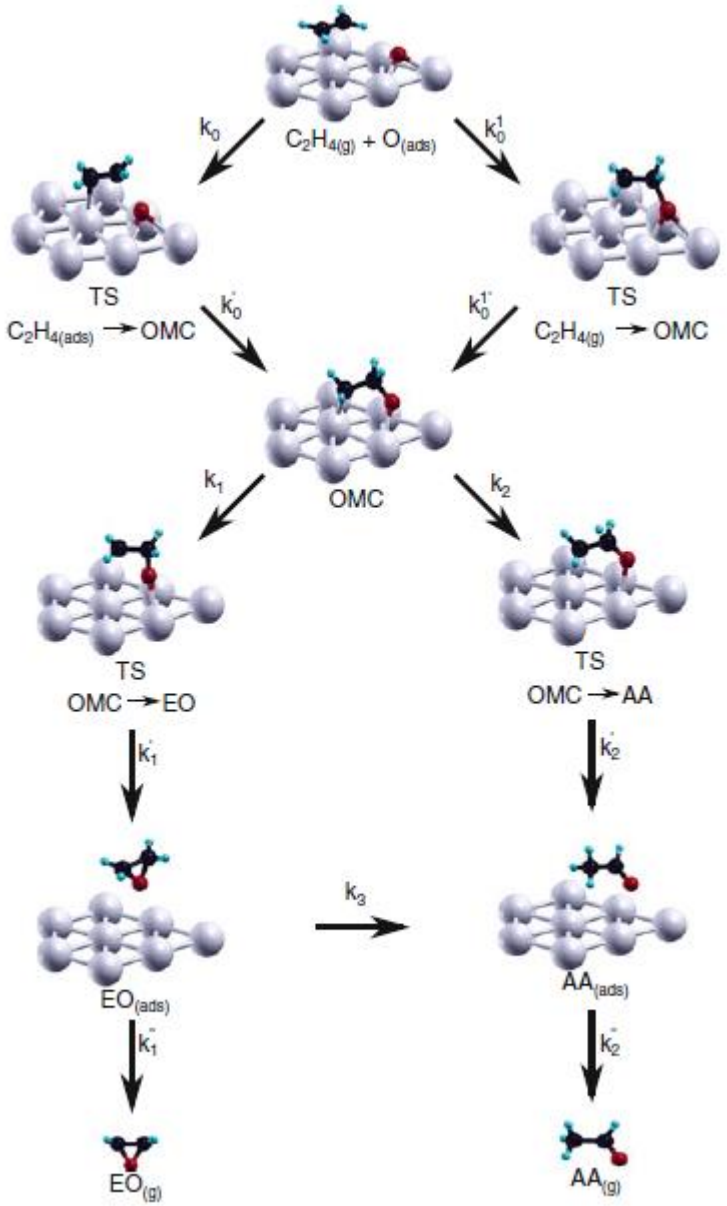

Figure 5. Possible mechanism showing the OMC intermediate as common precursor to EO and AA, reprinted from Özbek *et al.* [12].

Promoting metals

Özbek *et al.*[11] calculated that copper and gold oxides have a shift in chemical reaction barriers for the epoxidation reaction as compared to silver oxide because of their position in the periodic table. It is therefore expected that promoting silver with copper or gold would lead to a similar change in reaction barriers. It is however, not the aim to directly improve the catalyst with this promotion, but rather to create catalysts that can be useful for studying the behavior of oxygen. By in- or decreasing reaction barriers it might be possible to more clearly see changes in oxygen behavior, and this information could be used for the understanding of the mechanism.

In literature a lot of other promoting metals can be found. Cesium, rhenium or lithium are frequently mentioned in patent literature [28], [29]. The work of Jingfa *et al.* [30] showed that adding rhenium or cesium had a positive effect on both selectivity and conversion. In this work promotion with cesium will be considered. Synthesis procedures for catalyst with cesium promotion were optimized by Eline Hermans [31] and the catalyst with 10wt% Ag/Al_2O_3 and 750 ppm cesium were used. Activity test of this catalyst showed that for 750 ppm promotion and 1 ppm vinyl chlorine addition, the same selectivity but increased activity can be achieved as compared to the unpromoted catalyst. Synthesis methods for this catalyst can be found in the experimental section.

Chlorine

Chlorine is a moderator for the selectivity of ethylene oxide. However while it improves selectivity the overall reaction rate generally drops. Chlorine is introduced into the reaction using vinyl chloride, which adsorbs onto the surface and reacts with oxygen to form CO_2 and chlorine. Two main chlorine effects found in literature will be discussed here.

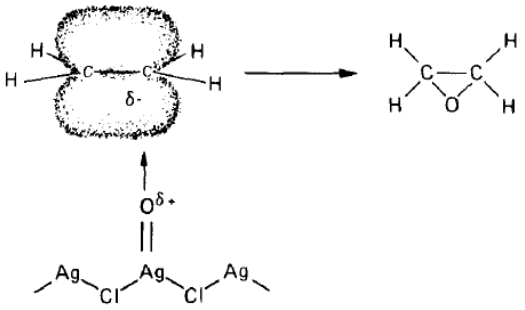

Figure 6. possible formation of electrophilic oxygen in presence of chlorine [27].

The effect of chlorine acting as a site blocker, proposed by Campbell *et al.* [4][5]. One of the effects is that the unselective reaction towards CO_2 needs more free silver sites than the selective route. When chlorine is added, it blocks a number of these sites and as a result slows down the unselective pathway. Chlorine also slows down the selective route but less harshly as compared to the unselective route.

Another possibility is that the electronic effect is more important. As explained in the section *''Oxygen''*, two types of oxygen can be distinguished on the surface, nucleophilic and electrophilic. Of these two types electrophilic is thought to create ethylene oxide. Van Santen *et al.* [27] have proposed that chlorine pulls electron density from oxygen and as such creates more electrophilic oxygen. In this process chlorine can still block silver sites, but the fundamental difference with the earlier effect is that chlorine also has an electromagnetic effect.

Particle size

Metal nanoparticle size is an important factor in any catalytic system as it affects a number of parameters. In order to explain these effects we will first assume a simple model of a spherical particle with a surface reaction. The changing parameter in this case is surface area. As the diameter of the particle doubles, its surface area will increase by factor four and its volume by factor eight. This means that per volume catalyst the amount of surface area, and therefore active sites, will decrease as particle size increases. Since the metals for most catalysts are expensive it is advantageous to have as much activity as possible per volume metal.

Another metal nanoparticle effect that is more specific for silver is that large nanoparticles have higher selectivity. Goncharova *et al.* [34][35] showed that there was a strong dependency between increasing particle size and selectivity towards EO formation on silver. The authors showed that this size dependency was most likely caused by changes in the surface sublayers. And that by increasing particle size certain crystal planes would be favored.

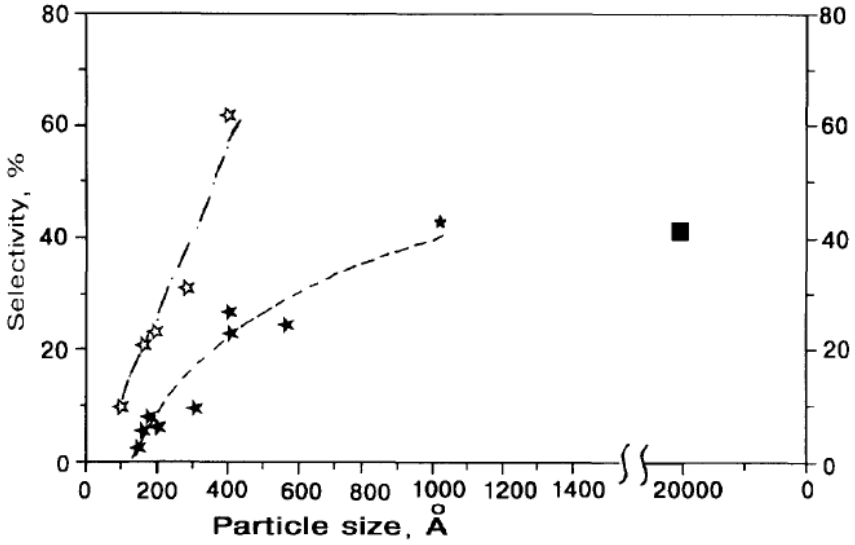

Figure 7. Silver nanoparticle size dependency of selectivity, graph from Goncharova *et al.* [34].

Metal nanoparticles are usually placed on support material. These supports are commonly porous materials in order to increase surface area. One of the advantages for a high surface area support is that more metal nanoparticles can be deposited in less volume, meaning that the catalyst as a whole has more activity per unit volume. This can be advantageous for reactor design as more activity per unit volume generally means smaller reactors which can save in construction costs.

In the case of ethylene epoxidation the product EO can isomerize to AA, which in the presents of active silver surface reacts towards CO_2 and water [14]. If EO is formed deep inside pores, it has to diffuse out. In this time EO is in contact with silver nanoparticle surfaces giving it a higher change of isomerization. Therefore low surface area α-alumina is used because it has low pore volume and minimal OH groups, which could cause isomerization.

Metal nanoparticle growth mechanisms

A catalyst's particle size is important for its functioning, however during heating or reaction this particle size can change. This process of changing particle size through heating or reaction is called sintering. Sintering itself can be divided into two main growth mechanisms: coalescence and Ostwald ripening. With coalescence two particles can gain enough mobility to be able to move towards each other and combine, creating one bigger particle.

Ostwald ripening is a process where large metal nanoparticles grow at the expense of smaller nanoparticles. This process occurs because atoms on the surface of a particle are less stable than atoms in the bulk. The surface atoms detach from their particles and diffuse in the continuous phase after which they can combine with another particle. The atoms on the surface of smaller particles are less stable than those of large particles, since the surface atoms in smaller particles have a lower average coordination number compared to large particles, due to relatively more edge and corner atoms. As a result large particles are energetically favored over small particles. Therefor with Ostwald ripening a large particle will grow at the expense of a small particle over time, whereas for coalescence two particles combine in a relatively short time. An example of these two processes can be seen in Figure 8.

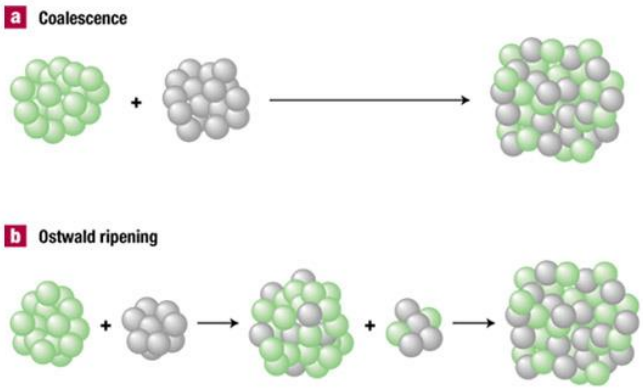

Figure 8. An example of Ostwald ripening and coalescence.

Scope of project

The scope of this project can be divided in two parts. The first part is to investigate the effect different oxygen coverages have on the ethylene epoxidation reaction. The second part will focus on the change in silver nanoparticle size during the epoxidation reaction.

From literature it is known that oxygen has a significant influence on selectivity in the ethylene epoxidation reaction [16] [19]. Several of the mechanisms debated in literature are explained in the sections ''*Reaction mechanism'','' Oxygen''* and *"Oxometallacycle mechanism*". In these mechanisms oxygen plays an important role. We will investigate the role of oxygen by approaching the function of oxygen using oxygen coverage. This is will be done by oxidizing silver supported catalysts to create a surface covered in oxygen after which ethylene is pulsed. These pulses are carried out in oxygen poor conditions to slowly move from conditions of oxygen rich to oxygen poor surface. TPD profiles and reaction products will be measured during pulsing to follow the dependency between oxygen coverage and selectivity. These reactions are carried out for different size particles and different dopants to determine if these affect the oxygen coverage dependency. The trends resulting from these samples can then be used to investigate the oxygen mechanism.

The second part of the project is focused on particle size and changes in particle size during reaction. From Goncharova *et al.* [34] it is known that for silver catalyzed ethylene epoxidation the particle size has a major effect on the rate of ethylene oxide production and selectivity. It is also known that it is common for metal particles to sinter and have changes in their particles size when exposed to heat and reaction[36]. For sintering several mechanisms are known as described by Thomas Hansen *et al.*[36]. In this project it will be investigated which mechanism is significant for particle size changes in the silver nanoparticle system. To do this a system is created where individual particle sizes can be tracked before and after reaction. This makes it possible to more accurately identify different sintering processes and hopefully give a better explanation for particle size changes in this system.

Experimentally, supported silver catalyst will be deposited on silicon nitride wafers with a window designed to be used for TEM. The particles on these wafers will be indexed using SEM and sufficiently good wafers will be indexed using TEM. After indexing, reaction will be carried out at industrial conditions of 225°C and 20 bar. After reaction the wafers will be indexed again by carefully keeping track of particles location. Individual particle growth can, in this manner, be tracked. From these experiments the process of particle growth, if any, can be elucidated. These experiments will also be carried out for catalysts with different particle sizes and cesium doping. The effect of the addition of a chlorine moderator on this process will also be explored. The results will be analyzed in a quantitative manner to be able to link the image data to on-stream experiments and selectivity data. A better understanding in catalyst deactivation can in the design of more stable catalysts.

Experimental

Catalyst preparation

Silver catalysts of several particle sizes were synthesized. Catalysts were doped with copper, gold and cesium. The following synthesis procedures are cited from the theses of Eline Hermans [31] and Shreyas Amin[37].

Pre-treatment of α-Al_2O_3

The α-Al_2O_3 used for catalyst preparation was sourced from Saint-Gobain NorPro. The sample code was SA 5102, which refers to 3 mm pellets of low surface alumina [38]. These pellets were crushed using mortar and pestle and then they were sieved to get particles in the range of 125-250 µm. We followed a pre-treatment procedure that involved washing the α-Al_2O_3 support with distilled water. Conceptually our washing procedure was similar to the one cited in the literature [39] where they used alumina monolith and washed it in boiling distilled water.

For our procedure, the crushed support was filled in a cellulose thimble and placed inside the Soxhlet equipment. A temperature controlled oil bath was used to boil the distilled water in the Soxhlet equipment and a cooling water was used to condense the vapors formed in the equipment. The alumina support was washed continuously with distilled water which was dripping due to the condensation of vapors from the top of the equipment. The catalyst sample chamber was completely filled with water in approximately 20 minutes and then it was emptied automatically by siphon effect. This entire procedure was allowed to continue for approximately 2 days (48 hours). Thus the cycle of washing the alumina support and emptying the water was repeated for approximately 150 times during the complete washing procedure.

After the washing procedure, the support material was dried at room temperature under vacuum for several hours and then at 110°C for 1 hour to remove any residual moisture and then it was stored for later catalyst synthesis procedure. Before proceeding for the synthesis of the bimetallic catalyst, the alumina support was heated and held overnight at 550°C to remove any organic impurities from the catalyst surface. [37]

Precursor solutions

Silver oxalate ($Ag_2C_2O_4$) was used as the silver precursor in all subsequent synthesis procedures. It was prepared by mixing silver nitrate ($AgNO_3$) (Alfa Aesar, 11414 Silver nitrate, ACS, 99.9+% (metals basis)) with excess of oxalic acid ($C_2H_2O_4$) (Sigma Aldrich, 241172 ALDRICH, Oxalic acid, ReagentPlus®, $\geqslant$99%) dissolved in distilled water and filtering out the precipitates. The precipitates were washed with water to remove excess acid and later dried in vacuum to remove moisture. [37]

Catalyst synthesis

Ag catalysts with various sizes were synthesized using the incipient wetness impregnation (IWI) method [40]. The prepared silver oxalate was slowly dissolved into an aqueous solution containing 3:1 M ratio of ethylene diamine to silver oxalate, according to the method reported by Diao et al.[41] The amount of silver oxalate was varied to achieve a loading of 2-10 wt% Ag and addition of caesium nitrate to achieve 0-1000 ppm Cs. All impregnation solutions were _lled up with deionized water until 1.6 mL reached and added to 2 g support. Optionally, the impregnated support was dried in a vacuum oven at room temperature for approximately 30 min before the catalysts were calcined under various conditions (medium, temperature and calcination time). [31]

Pulse setup

Pulse experiments were carried out in a quartz reactor tube inside a heating mantel. The catalyst was placed in the center of the reactor tube with quartz wool at both ends. Temperature was controlled using a thermocouple on the outside of tube with the tip placed close to the catalyst bed. Gas was flown through the reactor and analyzed by sampling the gas flow using a capillary connected to a differential pump. Part of this gas flow was sent to MS. A continuous gas flow was established through the loop, which could be switched to the reactor line in order to insert a certain gas volume. Precise pulse volumes of 10 µl, 100 µl and 1 ml were used. The reactor outlet was heat traced at 90 °C in order to prevent water condensation in the lines.

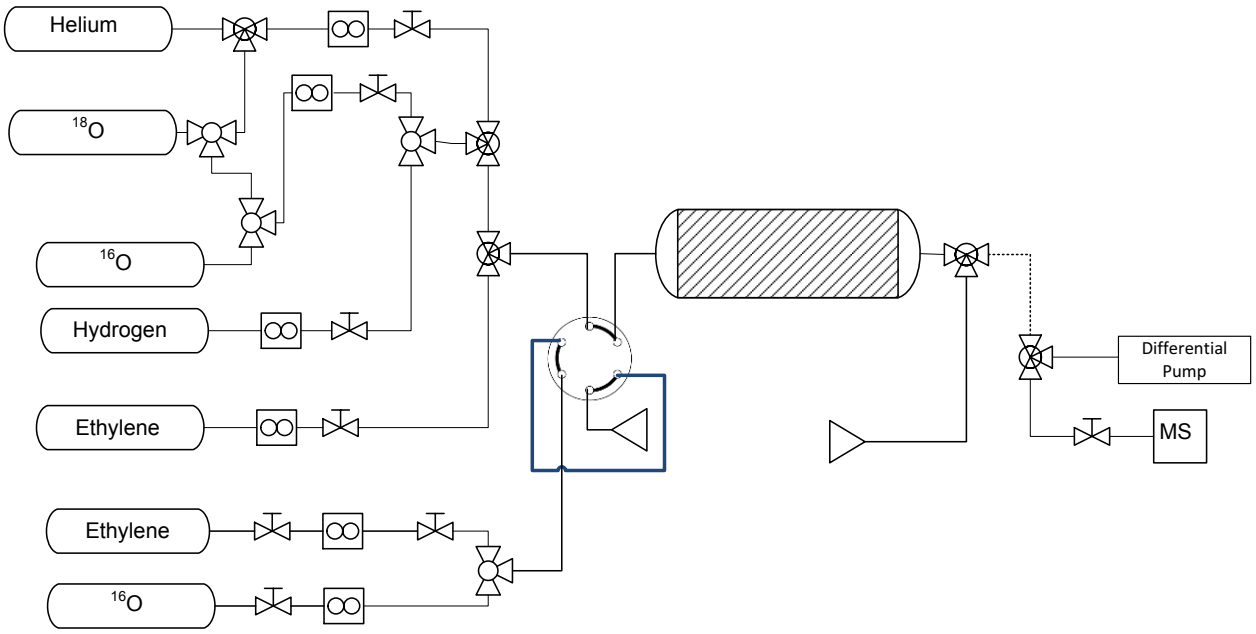

Figure 9. Schematic overview of pulse setup.

A typical pulse experiment used the following procedure. 250 mg of catalyst is loaded and pre-treated in pure O_2 (10 mL/min) at 250 °C. After 1.5 hours the temperature is lowered to reaction temperature (225 °C) and the system is flushed with He (50 mL/min) for 1 hour. Ethylene flow is established in secondary line (2 mL/min) through the pulse. Ethylene is pulsed using an automatic timing device (Multicomat RS 122-MH/ATX) at 200 second intervals. After X amount of pulses the pulses were stopped and temperature was lowered to RT. A TPD was carried out by raising the temperature at 10 °C/min till 550 °C. A schematic overview can be seen in Figure 10.

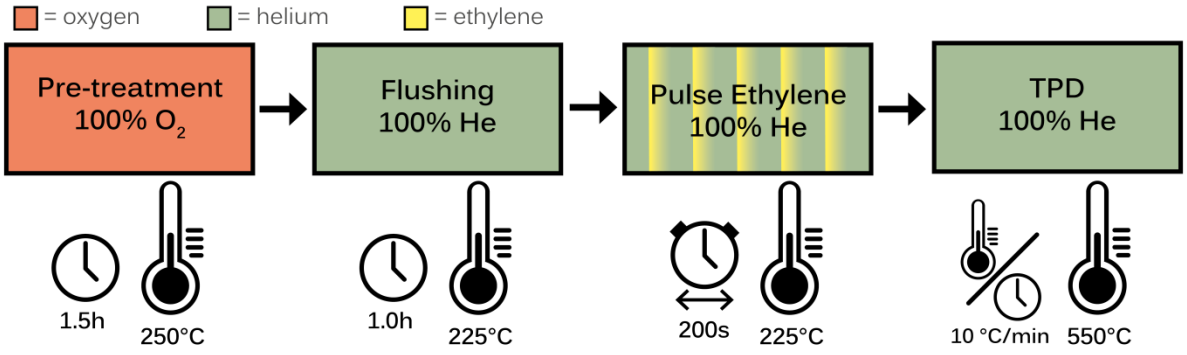

Figure 10. Schematic overview of a pulse experiment.

Processing

An in-house developed Matlab script was used to process MS-pulse data. Steps in the script include importing the data, creating a baseline, peaks integration and conversions from MS signal to absolute gas amount. In order to determine the sensitivity of the detector for each of the products, reference experiments were carried out. The pulse setup was loaded with Al_2O_3 support and was heated to reaction temperature (225 °C). Pure product gases (CO_2, ethylene, EO and O_2) were pulsed using 100 µL pulse. A more detailed description of the Matlab program can be found in appendix A.

The peak areas where plotted against the corresponding pulse number and smoothed with a Savitzky-Golay filter. All the data was normalized between zero and one in order to compare trends. Conversion and selectivity were calculated using equations 8 and 9. Note that these are ethylene conversion and EO selectivity.

$$Conversion = \frac{EO + \frac{CO_2}{2}}{Ethylene + EO + \frac{CO_2}{2}} * 100\% \quad (8)$$

$$Selectivity = \frac{EO}{EO + \frac{CO_2}{2}} * 100\% \quad (9)$$

TPD

In order to determine oxygen content of a catalyst a temperature programmed desorption (TPD) was carried out. The sample was cooled down from reaction temperature (225°) to room temperature and flushed with 50 ml/min of helium for 1h to clear the gas phase oxygen from the system. Temperature was raised at 10 °C/min to 550°C while helium flow was maintained. Gases were analyzed by MS. In order to quantify these results reference experiments were carried out where oxygen was pulsed using a 100 µl loop. Pulses were repeated 25 times and the experiment was repeated on another day. These values were averaged and using the ideal gas law the amount of moles oxygen was calculated.

In order to convert to monolayer oxygen equivalent it was assumed that oxygen would form Ag(I)oxide. In "The Handbook of Heterogeneous Catalysis" [40] a theoretical model was established for the determination of the dispersion for varying particle sizes. It first assumes the three lowest index planes of the crystal structure and uses crystal data to calculate n_s the number of surface atoms per surface unit. Next the volume of an atom in the bulk was calculated using equation 10. This was combined in equation 11 to calculate the final dispersion.

$$v_m = \frac{M}{\rho * N_a} \quad (10)$$

$$Dispersion = \frac{6 * v_m * n_s}{D_{particle}} \quad (11)$$

From theory it is known that multiple oxygen species exist in or on a silver nanoparticle. It is likely that these oxygen species have different binding energies and therefore will desorb at different temperatures, making it possible to detect them in TPD experiments. In order to give an indication of the presents of these oxygen species, peak fitting is applied. For each TPD two Gauss peaks were fitted. The results of these operations can be found in the results section.

Wafer deposition

Catalysts were deposited on round Si_3N_4 TEM wafers (Perfect Edge Si_3N_4 wafer, Smalltech supplies, window size 0.1 mm, membrane thickness 15 nm, diameter 3 mm). The wafer had a square window in the middle where it was only several nm thick. By depositing material in this area the electron beam of TEM could penetrate the wafer and images could be taken. Before deposition the wafer was cleaned with ethanol and dried at 100 °C for several hours. The catalyst was first crushed and then a small amount of catalyst (1-10 mg) is added to about 3 ml of ethanol. This dispersion was mixed, sonicated and immediately used. Wafers were put on a piece of filtration paper and 1 drop of solution was positioned on top, as such that the solution did not flow off the wafer. After 2-3 minutes another drop was deposited on the resting droplet in order to break surface tension and let most of the drop flow off the wafer. The resulting solution was left to dry in air. Wafers were initially screened using a Phenom Pro SEM (10 kV), after which suitable samples were indexed with TEM. An example of a wafer under SEM is given in Figure 11, note that the coloured boxes are zoomed in images taken by TEM. An overview of the wafers used is given in Table 1.

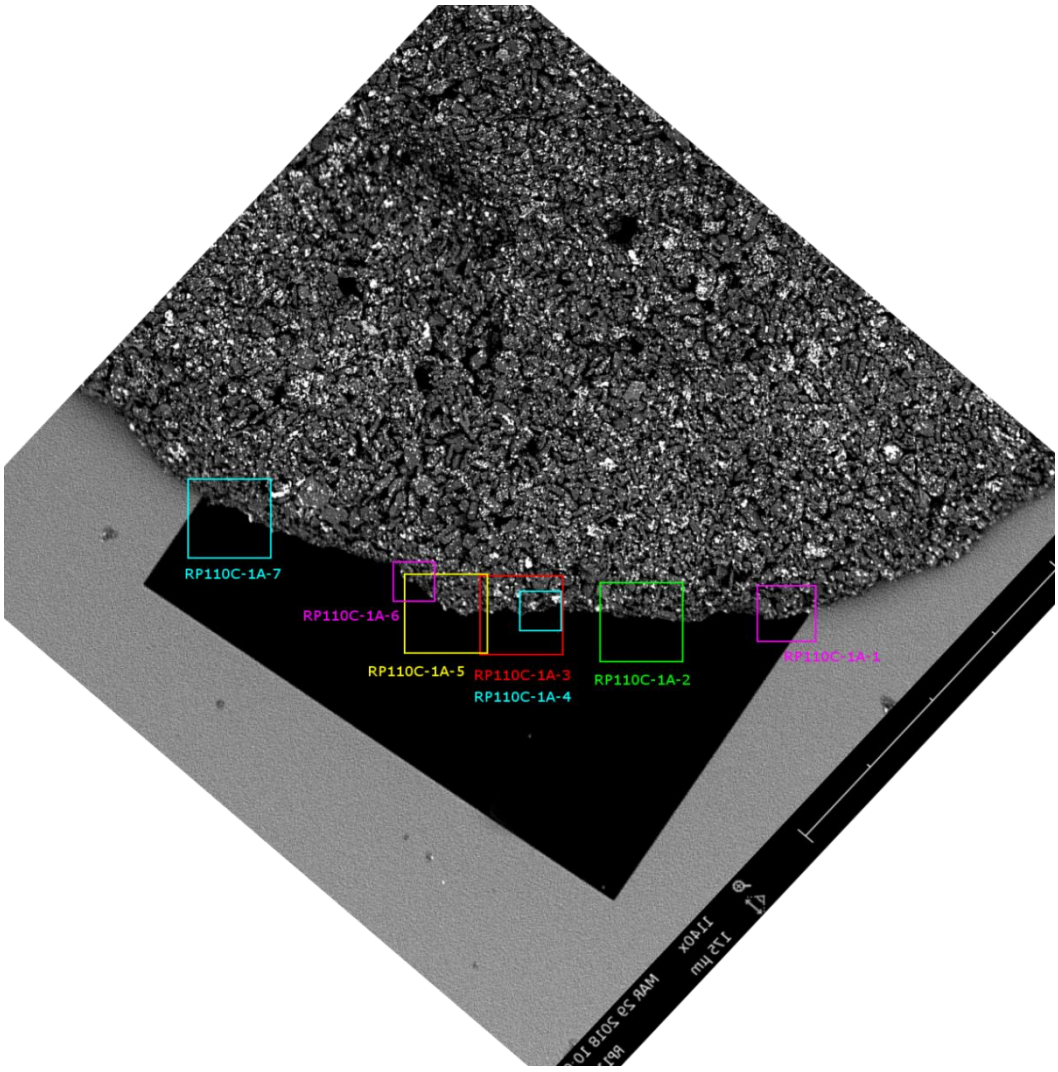

Figure 11. Example of SEM image of 10 wt% Ag on Al_2O_3, particle size = 100 nm (RP110C). Coloured boxes indicate locations of TEM images.

Table 1. Wafer samples with catalyst deposits.

Sample name	Catalyst name	Alternative name	Particle size [nm] +Promoting metal
RP96-C-	RP63	W1-Ag(128)	128
RP96-D-	RP63	W2-Ag(128)	128
RP103-D-	RP63	W3-Ag(128)	128
RP106-G-	RP104	W4-Ag(50)	50
RP110-A-	RP99	W5-Ag(100)	100
RP110-C-	RP99	W6-Ag(100)	100
RP110-E-	RP104	W7-Ag(50)	50
RP124-N-	RP63	W8-Ag(128)	128
RP127-A-	EH29	W9-Ag(110)/Cs	110 + Cesium
RP127-B-	EH29	W10-Ag(110)/Cs	110 + Cesium
RP128-D-	RP63	W11-Ag(128)	128

In the wafer results section samples will receive the suffix –image-[number] indicating that the information was from the same sample but taken from a different image.

Wafer analysis

In order to analyze TEM data, images were placed on top of each other using different layers in GIMP 2.10.2 (open sources graphic editing program). The images were rotated such that key support particles would align. By turning these two images into a GIF format it becomes much easier to spot individual differences between images. For quantitative analysis an area was marked out on the images in which all particles and different events were counted.

SEM

Scanning electron micrographs (SEM) were taken using the Phenom World Pro operated with an acceleration voltage of 10 kV. Samples were Si_3N_4 wafers with Ag/Al_2O_3 deposits. Images were used for further indexing under TEM.

STEM

Scanning transmission electron micrographs (STEM) were taken with the TU/e Sphera operated at room temperature with an acceleration voltage of 300 kV. Samples were Si_3N_4 wafers with Ag/Al_2O_3 deposits. Samples were used without an further processing steps.

TEM reactor

In order to carry out reaction on the wafers, a special TEM reactor was used. The wafers were placed in chambers in the reactor such that the surface of the wafers was open to the gas flow. The reactor was sealed and placed in a specially designed oven. A thermocouple was inserted into the metal

block of the reactor. Gases were flown continuously over the wafers at 20 ml/min at 20 bar. To start reaction the system was pressurized under an atmosphere of helium with 10% oxygen. When 20 bar was reached, the reactor was heated to 225 °C with an ramp rate of 20 °/min. This was held for 3 h of pre-treatment and 20 h, 40 h or 60 h reaction. Reaction gases were kept constant with 10% O_2, 5% ethylene and 85% helium with a total flow of 20 ml/min. Optionally 1% of 100 ppm vinyl chloride in helium was added. After reaction the reactor was cooled down to room temperature and flushed with helium.

Mass spectrometry

For analysis of the flow experiments mass spectrometry was used. The device used was a quadrupole mass spectrometer (Balzers QMG 420). Table 2 gives a summary of masses that were followed during reaction.

Table 2. Summary of masses and corresponding fragments measured by MS.

Mass	Fragment	Original species
15	CH_3^+	EO, Ethylene
16	O^+	Oxygen
18	H_2O^+	Water
28	$C_2H_4^+$	Ethylene
29	COH^+	EO
32	O_2^+	Oxygen
44	CO_2^+ , $C_2H_4O^+$	CO_2, EO

One of the species that is cross sensitive with the signals of EO is acetaldehyde (AA). Since AA is an isomer of EO it can be difficult to differentiate the two. However it is known that AA will burn completely to CO_2 and water in the presence of metallic silver [7]. Therefore it is unlikely that this substance will be produced in significant quantities.

Quantification

In order to couple the MS intensity to quantifiable units, reference experiments were carried out using pure gases. These were carried out for ethylene, ethylene oxide, CO_2 and oxygen. The following procedure was used: empty support was loaded into the reactor. The support was brought under helium atmosphere and heated to reaction conditions; this was left to stabilize for one hour. The substance in question was pulsed with a 100 µl pulse for a minimum of 13 pulses. These pulses were integrated and averaged. This value was used to convert MS intensity to gas volume which could be converted to mole using the ideal gas law.

Isotopes

In using MS, isotopes of different elements are a property that has to be taken in to account. In Table 3 the theoretical distribution for expected fragments is calculated. In this calculation the following isotopes in Table 4 were taken into account with their respective natural abundances. Of these isotopes it was found that only ^{13}C had a significant influence on the signals. The 29 m/z is most affected by this due to the ^{13}C of ethylene which can interfere. It was therefore assumed that

^{29}ethylene was the only significant interference on the 29 m/z signal, since the 28 m/z signal of ethylene is always two orders of magnitude bigger than the 29 m/z signal and the theoretical interference is around 2.25%, see Table 3. To compensate for this the 28 m/z signal of the corresponding experiment was taken and it was multiplied by the theoretical ratio between the ^{28}ethylene and ^{29}ethylene. This value was subtracted from the original 29 m/z signal.

When an isotopic labeled oxygen mixture was used, this consisted out of ^{18}O with purity greater than 97% (Eurisotop). For this oxygen mixture the theoretical distribution was also calculated and can be found in Table 3 marked as *iso*. This higher percentage isotope mixture is especially useful to resolve the 44 m/z signal. As EO only contains a single oxygen this will only shift 2 m/z while CO_2 will shift 4. Of course there is a chance that CO_2 will only have one ^{18}O and will have mass 46. This chance is calculated in Table 3 and is compensated for.

In order to calculate the change of an isotope being present in a molecule the following formula was used.

$$chance = \frac{n!}{k! * (n-k)!} * p^k * (1-p)^{n-k} * 100\% \quad 12$$

With *n* being the total number of atoms which can be the isotope, *k* the amount of labeled atoms and *p* the natural abundance. This formula consists out of two main parts. The first part:

$$\frac{n!}{k! * (n-k)!} \quad 13$$

Is used to determine in how many combinations the isotope can exist. For example take three books on a shelf. Two times book A and one times book B. It is not too difficult to imagine that these books can be arranged in three unique ways. And if the books were to be placed randomly all combinations would have an equal chance of coming up.

The second part of the formula is easier.

$$p^k * (1-p)^{n-k} \quad 14$$

To calculate the chance for a certain combination we revert back to our book metaphor. We want to calculate the chance for the sequence ABA. This means multiplying the chance for A twice with the chance for B, or more general as depicted in formula 14. If this is then combined with formula 13, it yields formula 12.

It must be noted that this calculation only takes into account the statistical chance of an isotope being built into a molecule. Energetic differences for the reaction with isotopes were not considered in this study.

Substance	Fragment	28 m/z	29 m/z	30 m/z	31 m/z	32 m/z	44 m/z	45 m/z	46 m/z	47 m/z	48 m/z	49 m/z
CO_2	CO_2						**98.50%**	1.10%	0.39%			
CO_2	CO	**98.66%**	1.14%	0.20%								
EO	C_2H_4O						**97.50%**	2.29%				
EO	COH		**98.64%**	1.16%	0.20%							
CO_2	CO_2 (*iso*)						0.09%		5.76%	0.06%	**93.06%**	1.03%
CO_2	CO (*iso*)	0.20%		**95.93%**	1.07%							
EO	C_2H_4O (*iso*)						0.20%		**94.88%**	2.11%	0.01%	
EO	COH (*iso*)		0.20%		**95.93%**	1.07%						
Ethylene	C_2H_4	**97.73%**	2.25%	0.01%								

Table 3. mass detection patterns for fragments resulting from different parent molecules. Empty spaces indicate values lower than 0.005%.

Isotope	Natural abundance
^{12}C	98.9%
^{13}C	1.1%
^{16}O	99.76%
^{17}O	0.04%
^{18}O	0.20%
^{1}H	99.99%
$^{2}H/D$	0.01%

Table 4. natural abundance of stable isotopes used in theoretical calculations in Table 3 [42].

Results & Discussion (Pulse)

A combination of pulse and TPD experiments were carried out in order to probe selectivity dependency of oxygen coverage. Pulse experiments were done to titrate the surface of oxygen and to obtain selectivity data as function of oxygen coverage. TPD experiments were used as supplement to pulse experiments to determine oxygen content in select situations. An example of a standard

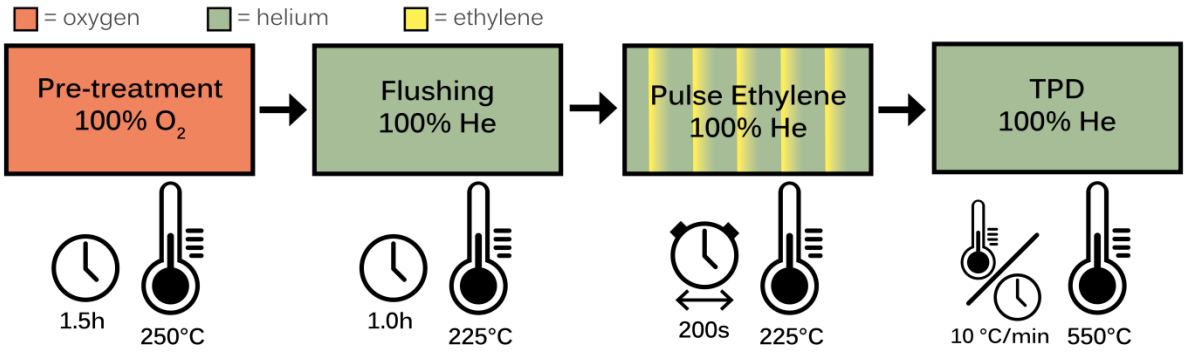

Figure 12. A schematic overview of pulse experiments.

pulse experiment can be seen in Figure 12. The first box left to right indicates a pre-treatment in pure oxygen for 1.5 hours at 250 °C. The second box is a flushing step to remove excess oxygen from the atmosphere. Then ethylene is pulsed at 100 µl depicted in the third box. The last step is optional and consists of a TPD profile in which first the system is brought to room temperature and then heated to 550 °C with a ramp rate of 10 °C/min.

Reaction temperatures

A temperature programmed reaction (TPR) was carried out to determine optimal reaction temperature for further experiments. 250 mg of 10 wt% Ag on α-alumina was loaded. The reaction was carried out under 10% oxygen in helium flow and 10 µl of ethylene was pulsed every 10 min. The temperature was raised with 15 °C/h, which equals with an increase of 2.5 °C per pulse. The integrated peak values as function of pulse number/time are shown in Figure 13.

An optimum for EO formation can be seen at around 265 °C, however for consecutive pulse experiments reaction temperature was chosen at 225 °C. This was done to run at lower conversion to prevent transport limitations from occurring and to prevent the CO_2 signal from overpowering the EO signal.

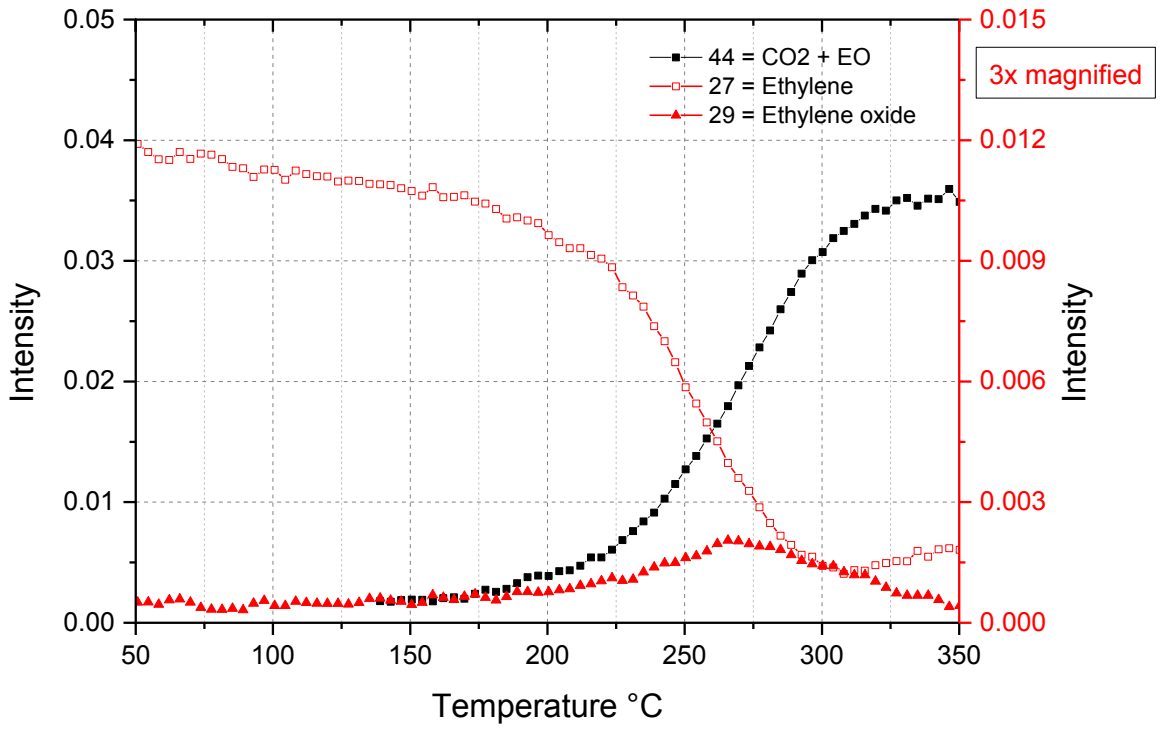

Figure 13. Ethylene pulse volume 10 µl, RT-->350°C at 15°/hr. Gas flow 40ml/min He + 5 ml/min O2. Experiment RP29, sample = SA00-a

Auto reduction of silver oxide

In literature it can be found that silver oxide can be unstable at elevated temperatures [43]. In order to determine the importance of this effect two experiments were carried out on silver powder. The powder was oxidized in pure oxygen at 250 °C, after which it was flushed with helium and ethylene was pulsed (10 µL). For the second experiment the time between pulses was doubled from 200 seconds to 400 seconds, the results can be seen in Figure 14.

It can be seen that the main peak shifts from pulse number 190 to 100, and that the total peak also seems compressed. This is likely due to the stability of silver oxides under higher temperatures. At elevated temperatures in the absence of oxygen, the absorbed oxygen will slowly desorb from the silver. In other words, besides reduction by ethylene, silver will also be reduced over time by at elevated temperature. Therefore if the pulse interval is doubled the, the time between each pulse is doubled and more oxygen is lost in this time. To circumvent this, the pulses are still continuously given while the oxygen coverage is decreasing, and therefore the reaction products are still produced at certain coverage levels.

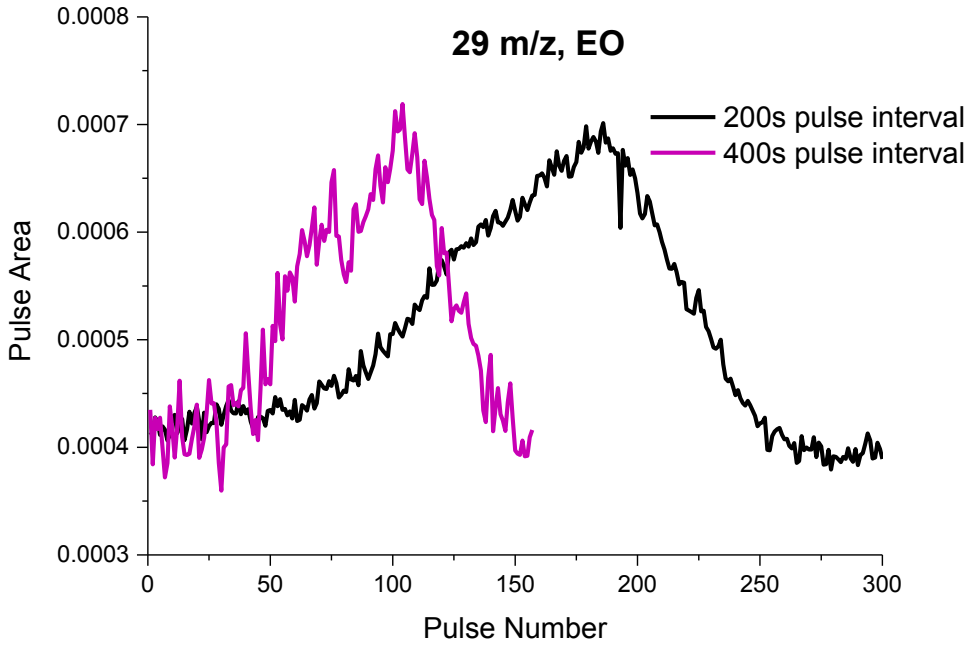

Figure 14. EO production during ethylene pulsing on pre-treated Ag powder produced through zinc synthesis. Influence of pulse interval.

Ethylene oxide without gaseous oxygen

The following experiments were carried out in order to see if a decrease in selectivity could be detected as a function of oxygen coverage. This experiment was carried out for three pre-treatment temperatures in order to establish whether this would have an effect. 250 mg of 10 wt% Ag on Al_2O_3 was pre-treated in pure oxygen at three different temperatures for 1.5 hours. The catalyst bed was flushed with helium (50 mL/min) and ethylene was pulsed (100 µL). The results can be seen in Figure 15.

From the 15 m/z and 44 m/z signal (Figure 15a & b respectively) it is observed that EO and CO_2 can be produced in the absence of gas phase oxygen. This is in line with results for the silver powder. Furthermore, the CO_2 is observable for longer than the EO signal. It can be concluded that as more pulses are given, the surface coverage decreases. Different pre-treatment temperatures did not affect the overall result. The determination of selectivity did not result in reliable data due to the low signal to noise ratio.

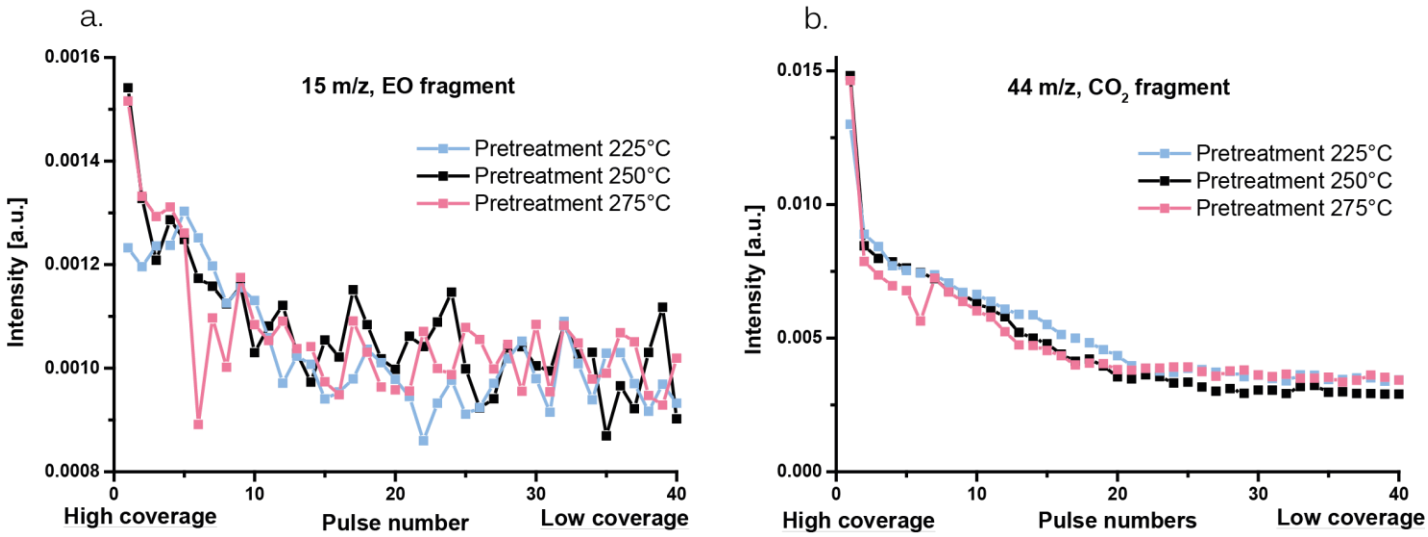

Figure 15. Integrated peak areas during ethylene pulsing (100% helium flow, 225 °C) over 10 wt% Ag/Al_2O_3 for a) EO and b) CO_2.Experiments RP58, RP59 & RP60 with sample = SA00-a.

Selectivity vs oxygen coverage

In the previous section "*Ethylene oxide without gaseous oxygen*" it was shown that when ethylene is pulsed the selectivity drops. For the next set of experiments the catalyst is oxidized during the pre-treatment and ethylene is pulsed again, however 1% of oxygen is added to the helium carrier flow to mimic reaction conditions.

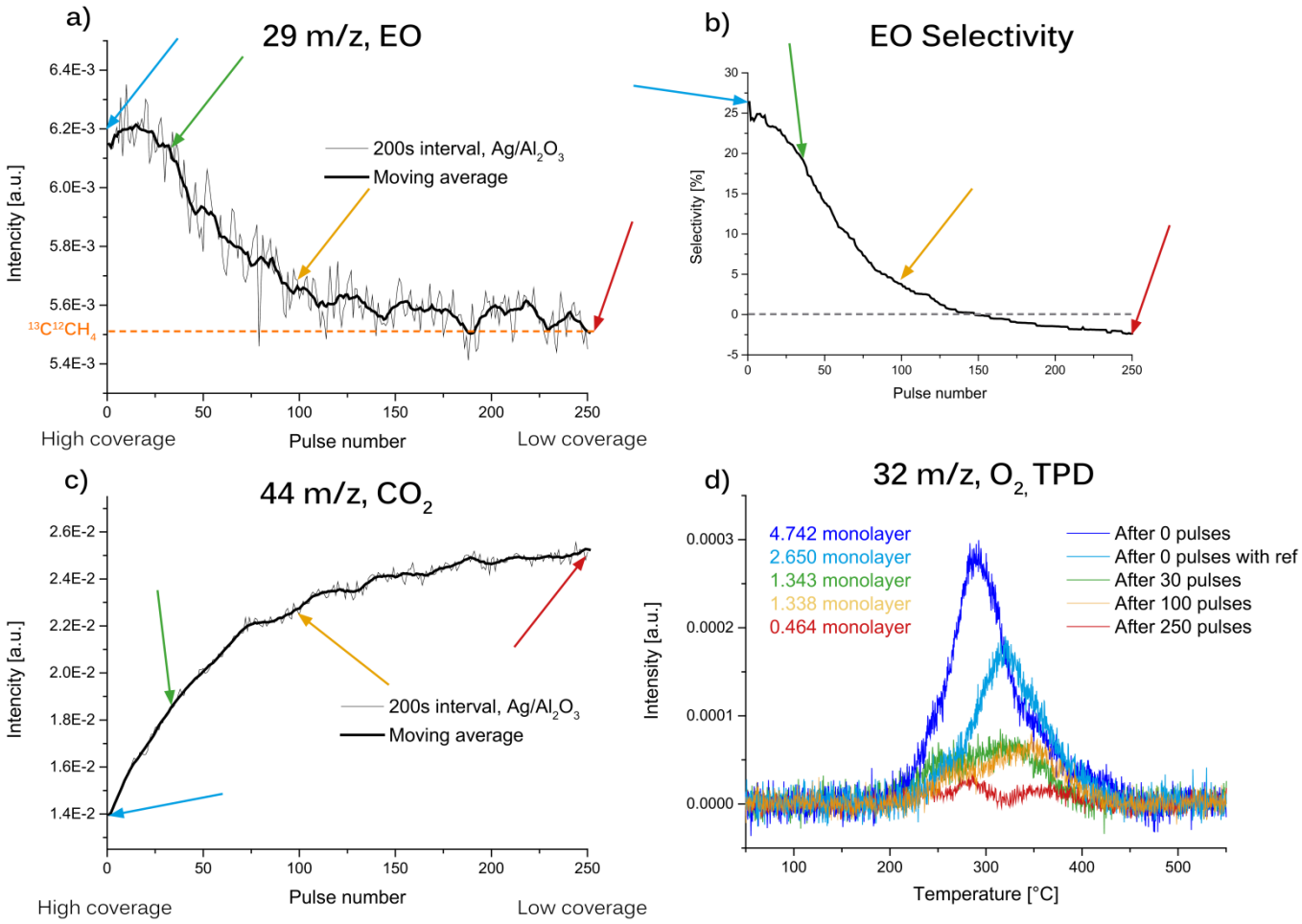

Figure 16. Ethylene pulse experiment with a flow of 50 mL/min He and 0.5 mL/min O2. Ethylene pulses of 100 µL are given every 200 s. **a)** 29 m/z signal of ethylene oxide, **b)** selectivity calculated from absolute gas amounts, **c)** 44 m/z signal of CO2, **d)** TPD's taken after different amount of pulses. TPD's were carried out by cooling down sample under oxygen atmosphere, flushing with helium and heating to 550 °C at 10 °C/min. Coloured arrows indicate time of TPD. Dark blue TPD was taken using the fastest TPD procedure, the light blue TPD profiles was taken under the same conditions as the remaining ones. Sample = RP63.

In Figure 16a the evolution of EO can be seen as function of pulse number. Here it can be seen that the signal for EO is initially high and decreases as function oxygen coverage. In Figure 16c the signal for CO_2 is seen to increase at the same time. This is in contrast to Figure 15a & b, where both EO and CO_2 production drop after 10 pulses. A possible explanation for this difference is the addition of 1% oxygen in continuous flow. The effect of this addition can be twofold. Firstly it could allow the catalyst to re-oxidize between ethylene pulses, in this manner the stripping of oxygen from the surface can be slowed down and be studied in more detail. The other effect is stability. Since silver oxides are unstable it was theorized that it is favourable to have a certain partial pressure of oxygen

present. This could ensure that the oxygen that is present on or under the surface remains stable and does not desorb.

It could be seen in Figure 16a & c, the signal for EO slowly decreases and the signal for CO_2 increases as function of pulse number. This also translates into the EO selectivity, seen in Figure 16b, which decreases. For this reaction TPD profiles were measured at 4 points indicated with the arrows. These TPD profiles can be seen in Figure 16d together with the calculated monolayer oxygen coverage.

The TPD profile for 0 pulses shows an amount of 2.65 monolayers oxygen present (light blue arrow). As more pulses are given the amount of oxygen in and on the catalyst decreases until the surface has almost no oxygen left for 250 pulses (red arrow). At this point no detectable amounts of ethylene oxide are produced and the only product is CO_2. However the results of the TPD experiments are not the actual coverages at a given amount of pulses. Rather it is an amount of oxygen that is at least on the catalyst. This is due to the way the TPD profile has to be measured. In order to measure a TPD profile, the temperature of the system is lowered to RT. To minimize the amount of auto reduction (which occurs at elevated temperatures) flushing with He was started at RT, however oxygen desorption during cooldown and flushing cannot be completely excluded. Therefore, TPD profiles at certain time-points in the experiment are the most accurate indication for oxygen coverage.

In Figure 16b there is a significant drop in selectivity between pulse 30 and 100. However, the TPD profiles of 30 and 100 pulses have nearly the same values. This makes for two schools of thought. The first is that since the TPD profiles are the same the oxygen coverage at these two points must be the same and this decrease in selectivity is not caused by the decrease in oxygen coverage.

The second possibility is that the oxygen lost during flushing does not scale linearly with total amount of oxygen. For example, we take a situation A with 80 oxygen present and situation B with 50 oxygen present. Flushing starts and A very quickly loses 30 oxygen after which it slowly loses 10 more. B on the other hand only slowly loses 10 oxygen. Both A and B will, at the end, only have 40 oxygen left and this would be measured by a TPD. For the TPD profile for 30 and 100 pulses this process could have occurred. This would mean that the selectivity loss in this area was caused by a decrease in oxygen coverage. The possibility of oxygen coverage causing the drop in selectivity in this domain will be further discussed in the section “TPD fitting”.

It should be noted that in Figure 16a the signal for EO, 29 m/z, does not trend towards zero, but rather towards approximately 5.5e-3 intensity. This is the signal of ethylene with one ^{13}C present. This value of 5.5e-3 matches the theoretical value which would be expected if the 28 m/z signal is multiplied by the chances for ^{13}C ethylene calculated in the theoretical section. For the selectivity calculation this value is subtracted from the 29 m/z signal. However some inaccuracy of a few percent remains, which is why the calculated selectivity is slightly negative with a few percent.

Monolayer oxygen equivalent

It should at this point be noted that for the calculation of oxygen coverage use is made of monolayer oxygen equivalent (MOE) calculation as explained in the experimental section. However this yields coverages of well over 1, meaning that oxygen has to be present in another form than surface Ag(I)oxide. A reference TPD was also carried out with empty support which yielded no oxygen peak.

One of the options is that silver could have a higher oxidation state, however this is very unlikely as silver(II) and silver(III) states are unstable and require a very strong oxidizing agent in order to form. When the MOE is taken, one can reverse the formulas to calculate how big a particle should be to fit

1 monolayer at this maximum. It was found that the highest oxygen coverage is present using a pre-treatment of 250 °C, see Figure 17 and Table 5, resulted in a MOE of 4.7. If this amount of oxygen is set to be 1 monolayer the theoretical particle size was calculated to be approximately 30 nm.

Peak broadening of XRD can be used to determine the crystallite size by using the Scherrer equation. The result of this was crystallites of around 30 nm. This could mean that the large silver particles consist of multiple crystallites connected up via grain boundaries. Subsurface oxygen could then be present at these grain boundaries and explain where the extra oxygen is coming from.

Pre-treatment

TPD experiments were carried out to probe if the oxygen content of the catalyst could be influenced. By influencing the oxygen content it was expected that the selectivity in subsequent experiments could be influenced. The results of the TPD experiments can be found in Figure 17. From these TPD experiments absolute oxygen content was calculated which can be found in Table 5. Both the values for the monolayer equivalent and crystallite model are given. It can be seen that for different pre-treatment temperatures an optimum exists with respect to oxygen content. This optimum lies at 250 °C where the oxygen content is 4.7 times monolayer coverage.

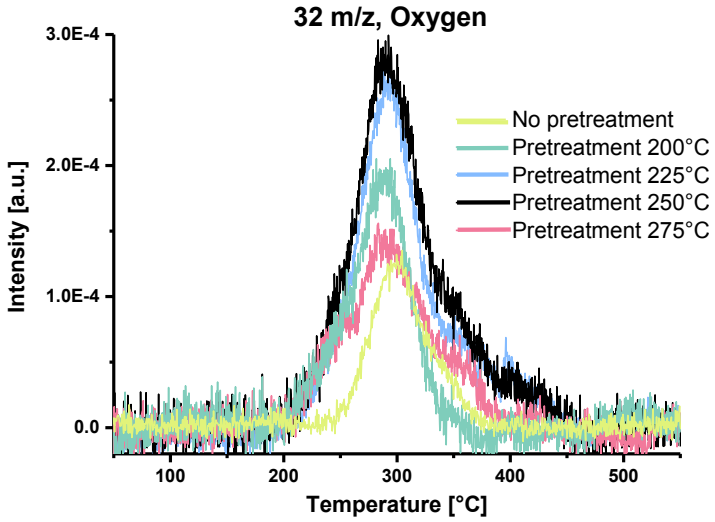

Figure 17. TPD for different pre-treatment temperatures, no ethylene pulses. Sample = RP63.

Based on the TPD data it was expected that differences in selectivity could be observed during pulse experiments. Namely, if the pre-treatment was carried out at a different temperature, the pulse experiments would start with different oxygen content. The results of these pulse experiments can be seen in Figure 18. There are differences between pre-treatment temperatures, but no clear correlation. It is possible that due to a low signal to noise ratio, no trends could be observed here.

Table 5. Oxygen amount detected with TPD for different pre-treatment temperatures

Pre-treatment	Monolayer equivalent	Crystallite model
RT	1.5	0.3
200 °C	2.4	0.6
225 °C	4.0	0.9
250 °C	4.7	1.1
275 °C	2.5	0.6

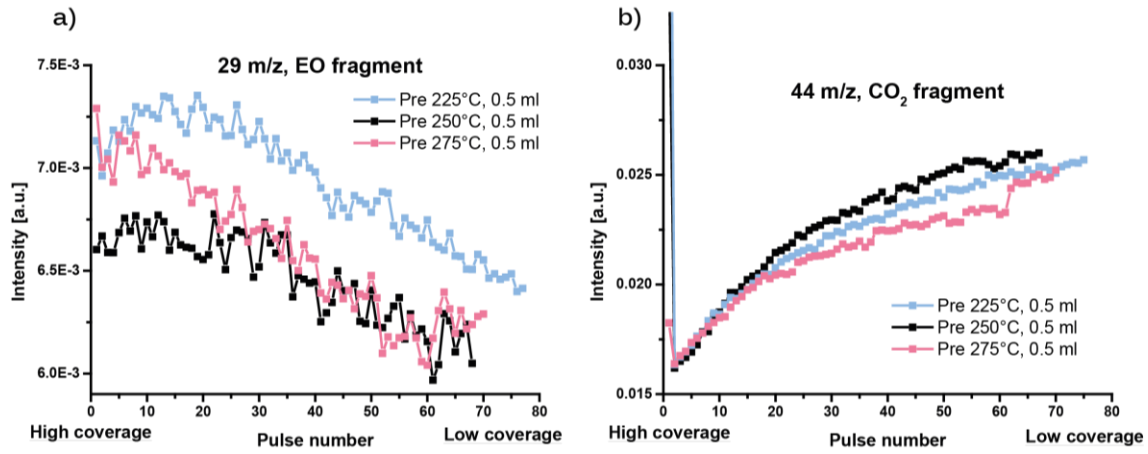

Figure 18a & b. Ethylene pulses in 50 ml/min of He and 0.5 ml/min O_2. **a)** 29 m/z for COH^+ fragment. **b)** 44 m/z for CO_2^+ fragment or $C_2H_4O^+$ fragment for EO. Experiments RP72, RP74 & RP75, sample = RP63.

TPD fitting

Peak fitting for TPD experiments was carried out. For pre-treatments in the range 200-275 °C the first peak lies at around 285 °C with relative consistency. For pre-treatments there is an optimum at 250 °C for the area of the first peak, which is also the main contributor for the optimum for the total area. For TPD's after different pulse amounts, area 1 declines very fast after zero pulses and for 100 and 250+ pulses remains stable. As described in an earlier section the total area difference of 30 and 100 pulses is very small. This while at the same time pulse experiments show a big decline in selectivity. It is for the moment assumed that the absolute amount of oxygen in these situations is the same and that the same amount is lost as unmeasured oxygen. While the total amount of oxygen doesn't change, the composition does. It can be seen in Table 6, that changing from 30 to 100 pulse, the amount of area 2 increases while area 1 decreases. So the drop in selectivity could be caused by this change in oxygen species on the catalyst. This conclusion lies in line with the work of Schlögl [25] who showed using XPS that selectivity changed simultaneously with the change in nucleophilic and electrophilic oxygen species.

Table 6. Results of peak fitting. X1 and X2 are x positions of the first and second peak. Area 1 and 2 are integrated areas of fitted peaks, with Area Total the sum of both areas. Fitting of RP60 resulted in 1 peak being more accurate than 2.

Name	Description	X1[C°]	X2[C°]	Area 1	Area 2	Area Total
RP60	pre-treatment 200 °C	284		0.074		0.074
RP58	pre-treatment 225 °C	289	325	0.065	0.077	0.142
RP51	pre-treatment 250 °C	290	368	0.120	0.029	0.149
RP59	pre-treatment 275 °C	290	363	0.076	0.004	0.080
RP81	No pre-treatment	298	345	0.040	0.006	0.046
RP122	after 0 pulses	321	392	0.084	0.005	0.089
RP121	after 30 pulses	255	327	0.018	0.028	0.045
RP123	after 100 pulses	266	341	0.009	0.033	0.042
RP120	after 250+ pulses	275	366	0.010	0.005	0.014
RP130	Copper promotion	250	340	0.002	0.052	0.054

Fitting of this data was done based on the work of Schlögl *et al.*[25] and Van Santen *et al.*[24][27]. According to this literature the most likely case of that two kinds of oxygen are present and can be fitted. More details about the different kinds of oxygen can be found in the section "Oxygen". It is acknowledged that fitting with three or four peaks is also valid in some cases and that due to the small dataset there is a portion of uncertainty in these results. Figure 19 shows an example of a fitted TPD experiment.

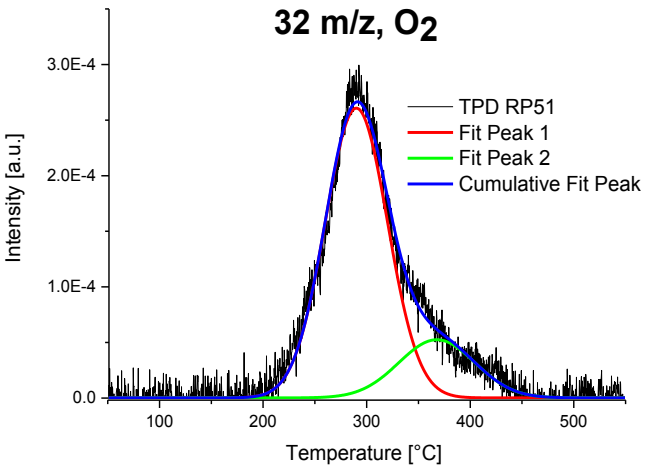

Figure 19. Fitted oxygen TPD of RP51.

Pulse interval

Pulse intervals were varied to see if this would affect the results. When the pulse interval is increased to 400 and 800 seconds the trends remain largely the same, as can be seen in Figure 20. This firstly shows that the addition of 1% oxygen to the flow supresses the auto reduction of silver oxide. As was shown in earlier experiments, see Figure 14, when no oxygen is added and pulse interval is doubled the resulting response is compressed in time by a factor two. Since the experiments with 1% do not show this compression it can be concluded that this oxygen loss is supressed. The experiments in Figure 20 also show that the silver does not re-oxidize in a significant manner as a result of 1% oxygen. If this was a significant factor, one would expect the experiment with an 800 seconds interval to have a slower decline in EO production, as the silver has more time to recover its oxygen content between pulses.

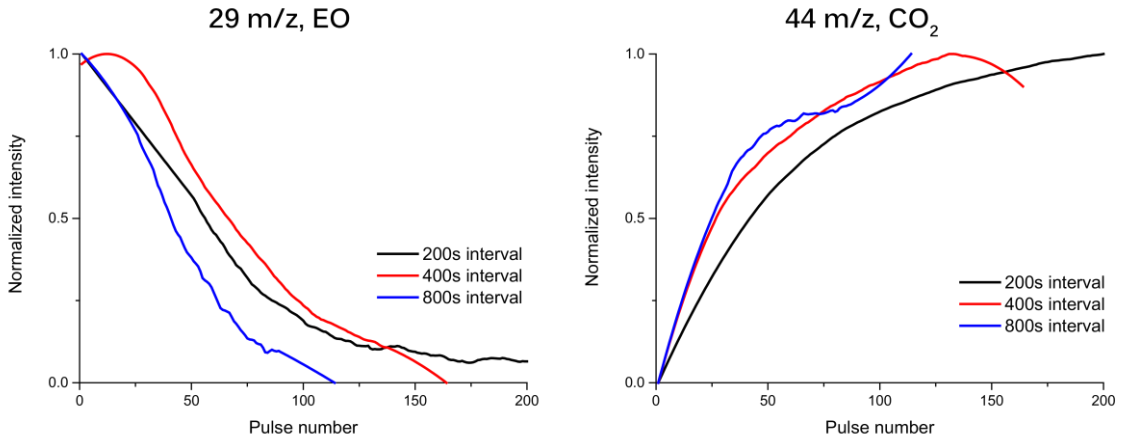

Figure 20. Pulse experiments for pulse intervals of 200, 400 and 800 seconds. Experiments RP72, RP96 & RP98, sample = RP63.

Copper and gold promotion

Silver catalyst was promoted with gold and copper in order to change the oxygen binding energy and reactivity. By adding these promotors the energy of reaction barriers could potentially be changed and this can perhaps reveal interesting behavior concerning oxygen.

The copper sample used was SA05 provided by Shreyas Amin [37], the sample contained 1500 ppm of copper. The same pulse experiment was carried out as for unpromoted silver were copper was first oxidized and then ethylene was pulsed over it, see Figure 21. Note that in order to compare the results, they had to be smoothed and normalized. The selectivity given is calculated using the normalized data seen, meaning that selectivity will run from 100% to 0%.

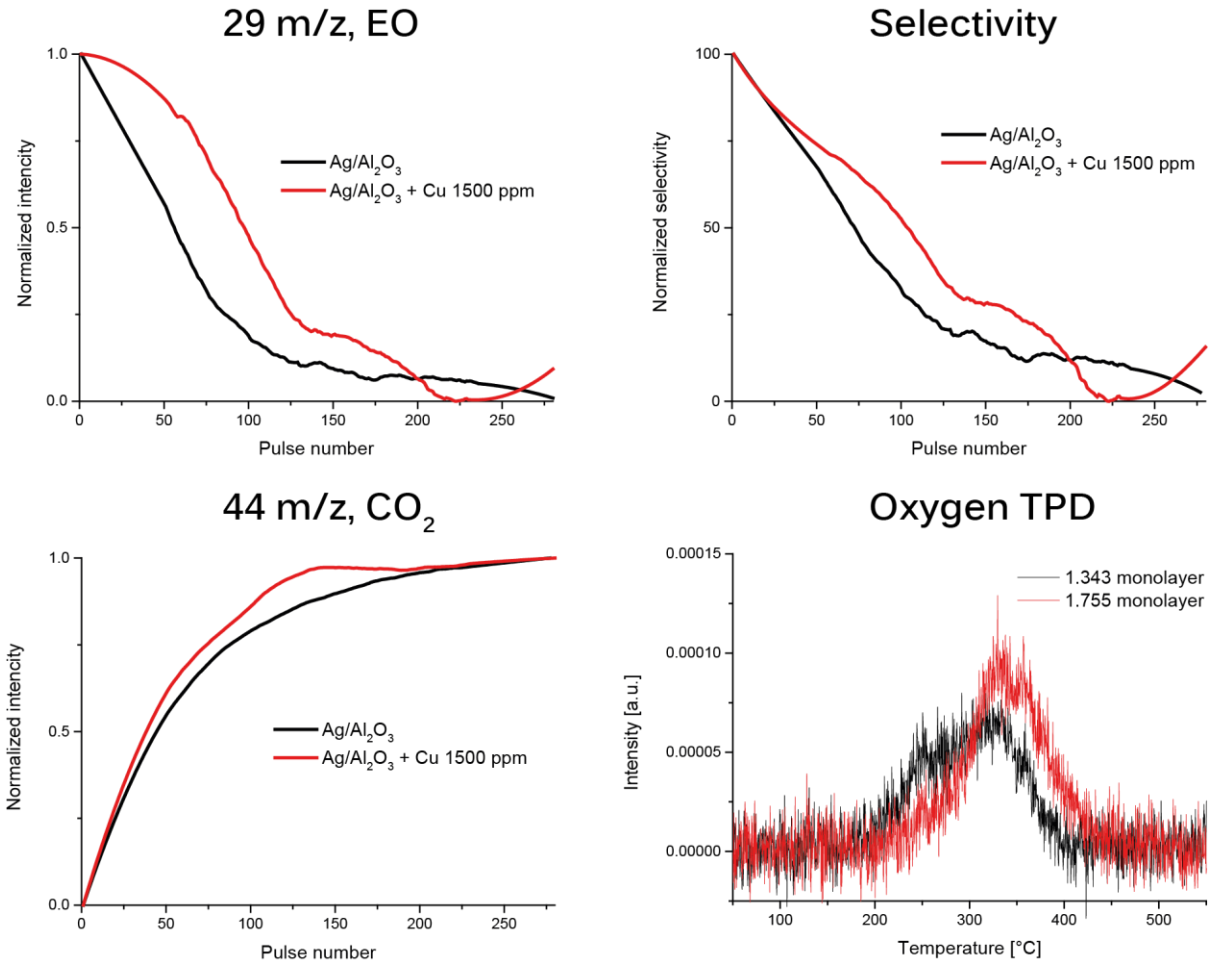

Figure 21. Normalised pulse experiments of 10wt% Ag and 1500 ppm Cu on 10wt% Ag. TPD taken at 30 pulses. Experiment RP72 & RP111. Samples RP63 & SA02.

In order to compare whether oxygen coverage decreases at an equal rate, a TPD experiment was carried out after 30 pulses for both samples. This resulted in the monolayer values also seen in Figure 21. The coverage of copper at this instance is approximately 30% higher than unpromoted silver. This could be the reason for the higher selectivity of the copper promoted sample. The lower coverage could be explained in several possible ways. Firstly, it is an effect of reduced conversion. Copper promotion could have reduced the number of active sites by blocking leading to a reduced conversion rate, leading to less oxygen being used for each pulse. This could be check by measuring the conversion; however these measurements were not sufficiently accurate to say anything conclusive.

Another possibility is that copper enhances the re-oxidization which allows the catalyst to regain more oxygen in between pulses. A third option is that copper changes the surface in such a way that the more selective type of oxygen is stabilized longer. This would be in line with the conclusions made in the section “Monolayer oxygen equivalent” which state that between 30 and 100 pulses the change in selectivity is more likely caused by a change in oxygen type rather than absolute amount.

The samples with gold doping did not have enough activity to carry out measurements with a high enough signal to noise ratio. This is probably due to the presences of chlorine in the samples, as this was used to synthesize the catalyst. Chlorine is known to increase selectivity for silver catalyst but also to drastically decrease activity. Details on this problem can be found in the thesis of Shreyas Amin[37].

Selectivity effect of particle size

When changing particle sizes a few crucial parameters change. In this case it was chosen to keep surface areas constant. To achieve this is was necessary to change metal loadings, in analysing the results this is considered.

In Figure 22 it can be seen that the 95 nm and 129 nm particles are quite similar in their pulse behaviour. However the small particles have a much faster decline in EO production. This can be related to the amount of oxygen that is present in the catalyst. The rate at which the EO signal declines indicates that the oxygen that was present, is used up more rapidly as compared to a large particle.

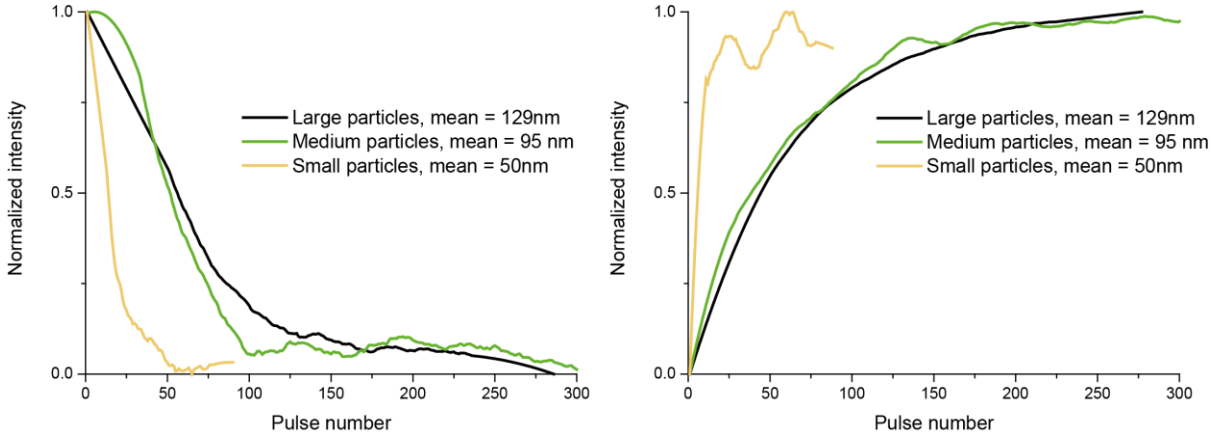

Figure 22. Pulse experiment carried out for different particle sizes. Large particles = 129 nm, medium particles = 95 nm and small particles = 50 nm. Experiments RP72, RP105 & RP107.

From TPD experiments, Figure 23, it is known that smaller particles hold less oxygen reserves under the same conditions even though the surface area of these particles per gram catalyst was calculated to be the same. However the TPD profile only shows the absolute amount of oxygen released. In synthesizing smaller particle sizes it was necessary to change the metal loading in order to obtain the desired particle sizes. This makes that in comparing oxygen coverages there needs to be compensated for weight loading and particle size. This was done in Table 7 where the integrated area from the TPD seen in Figure 23, was converted to Ag_2O monolayer equivalent. In order to compare these catalysts, values for oxygen content per amount silver were also calculated. In this calculation it was taken into account that particles had different loading and particle size.

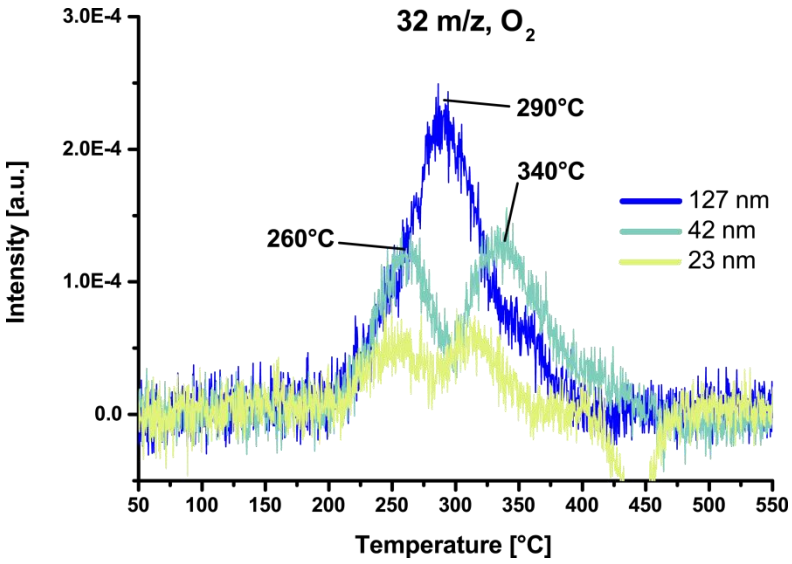

Figure 23. TPD measurement of three different particle sizes. Samples were oxidized in pure oxygen for 1.5 h at 250 °C. Experiments RP52, RP53 & RP54.

In Table 7 it can be seen that the smallest particles (RP54) have the highest amount of oxygen per gram of silver. However both the small particles (RP53 and RP54) have adjusted monolayer coverages of around 1. This monolayer model is still based on Ag_2O which could mean that the small particles have less or no subsurface oxygen, but only a surface covered in Ag_2O. The reason why only large particles would have subsurface oxygen could be explained by grain boundaries. As explained in the section "Monolayer oxygen equivalent", for large particles XRD showed that the crystallite size is around 30 nm, meaning that large particles consist out of multiple crystallite areas. For small particles it is possible that these grain boundaries do not exist because the particle is too small to support it. And as a result, small particles do not have subsurface oxygen. This could be the explanation for the size effect in silver for the epoxidation reaction. Because small particles do not have grain boundaries, they do not have subsurface oxygen and as a result do not have the selectivity that large particles have.

Table 7. Surface coverages of varying particle sizes corrected for loading and particle size. Monolayer equivalent assumes a surface of Ag_2O.

Name	Particle size [nm]	Loading [wt%]	Monolayer equivalent particle size and loading corrected	O_2 per Ag [µmole/g]	O_2 per gram catalyst [µmole/g]
RP51	127	10	4.7	197	19.7
RP53 (EH19)	42	10	0.96	115	11.5
RP54 (EH34)	23	2	1.1	266	5.3

Conclusion pulse

In order to investigate the oxygen mechanism in the ethylene epoxidation reaction an experiment was setup to measure selectivity as function of oxygen surface coverage. A silver surface was fully oxidized with oxygen after which ethylene pulses were used to titrate the surface and measure selectivity. It was shown that it is possible to carry out experiments where oxygen coverage is slowly decreased and that selectivity measurements can be taken. This is done by having a low concentration of oxygen in continuous flow after initial oxidation and pulsing with ethylene. By increasing the pulse interval time in presence of low oxygen concentration, the results as function of pulse number did not change. This means that low oxygen concentration prevents oxygen loss by other processes than pulsing.

The general trend was that for decreasing oxygen coverage the selectivity also decreases. The decrease in oxygen coverage can be followed with TPD profiles and shows a decrease of 4.7 monolayer equivalent to 0.5. Using XRD data and catalyst with smaller particle sizes, it was concluded that a large part of oxygen is present in the subsurface. This shows that if theoretical models of this system are to be undertaken, that this oxygen should be modeled very carefully.

TPD profiles were fitted using a two type oxygen model. During the decrease of selectivity the composition of oxygen changed, therefore it is likely that the nature of oxygen also influences that selectivity of the reaction.

The addition of copper changes the selectivity during pulse experiments. Combined with the TPD data of copper it is possible that the change in selectivity that copper induces, comes from the change in stabilization of different oxygen species.

For small particles the selectivity drops very quickly upon pulsing. This is due to less oxygen per gram catalyst, which in turn is because smaller particles have less to no subsurface oxygen.

Results & Discussion (Wafers)

By depositing Ag/Al_2O_3 powder catalysts on Si_3N_4 wafers a system was created in which *in situ* particle growth and change could be followed using TEM. Combining this with a high-pressure TEM-wafer reactor allowed us to track individual silver nanoparticle growth and structural changes within multiple areas of the support. Where other methods for the determination of particle size use averaged values, this method analyzes particles on a particle by particles basis. The aim of this method is to more accurately determine what growth mechanisms or processes are responsible for particles size changes.

Events

TEM images of different reaction stages were compared to each other. It was clear from the images that several processes or events can take place. However, showing a single instance of an event does not mean anything, since this can still be coincidence. Therefore a more systematic approach is needed. First the TEM images will be investigated and different events will be found. Next these events will be classified into different groups. This section will be dedicated to identifying and categorizing these events into groups. After a list of events is made, the events can be counted and the results can be quantified.

Coalescence (combination)

In the case of coalescence two particles in close proximity merge into one. An example of this can be seen in Figure 24 indicated by the red circle. In logging the events a coalescence event between two or more particles will be logged as 1 event. In analyzing the data it was found that small particles are more likely to coalesce as opposed to large particles. This can also be found in literature were according to Hansen *et al.*[36] larger particles are less mobile and therefore less likely to coalesce.

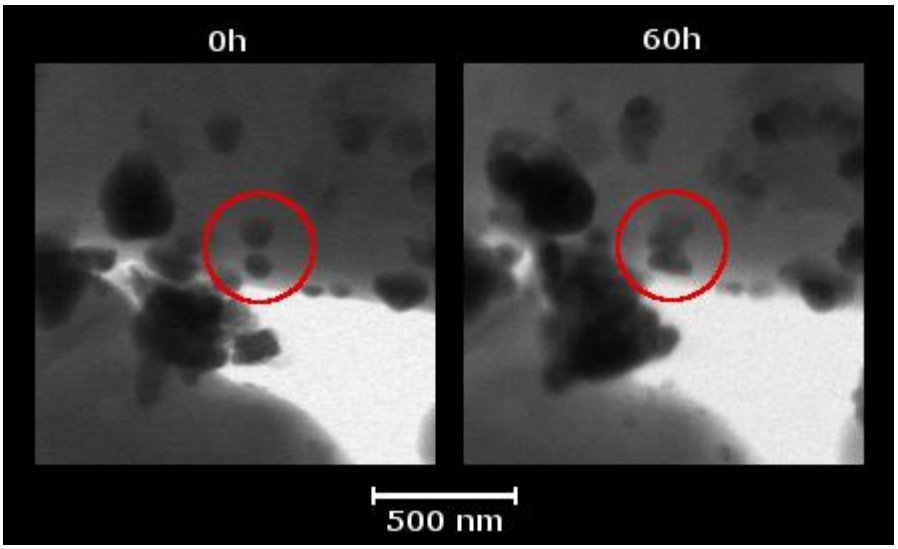

Figure 24. Coalescence of two silver particles supported on α-alumina marked by red circle.

Mechanical loss

Mechanical loss can occur for all samples and is unrelated to particle growth. It simply means that pieces of sample break of or just fly away. Since the Al_2O_3 support is not chemically bonded with the Si_3N_4 wafer they can break off. This can happen during transport or loading of the sample, but it can also happen as a result of charging. As the wafer itself is not conductive, charging can become a major issue when too large a zoom is used in TEM. It should also be taken into account that areas surrounding an area that has broken of needn't be representative of for example Oswald ripening or other area effects and caution should be taken in analyzing these areas. An example of the process can be seen in Figure 25.

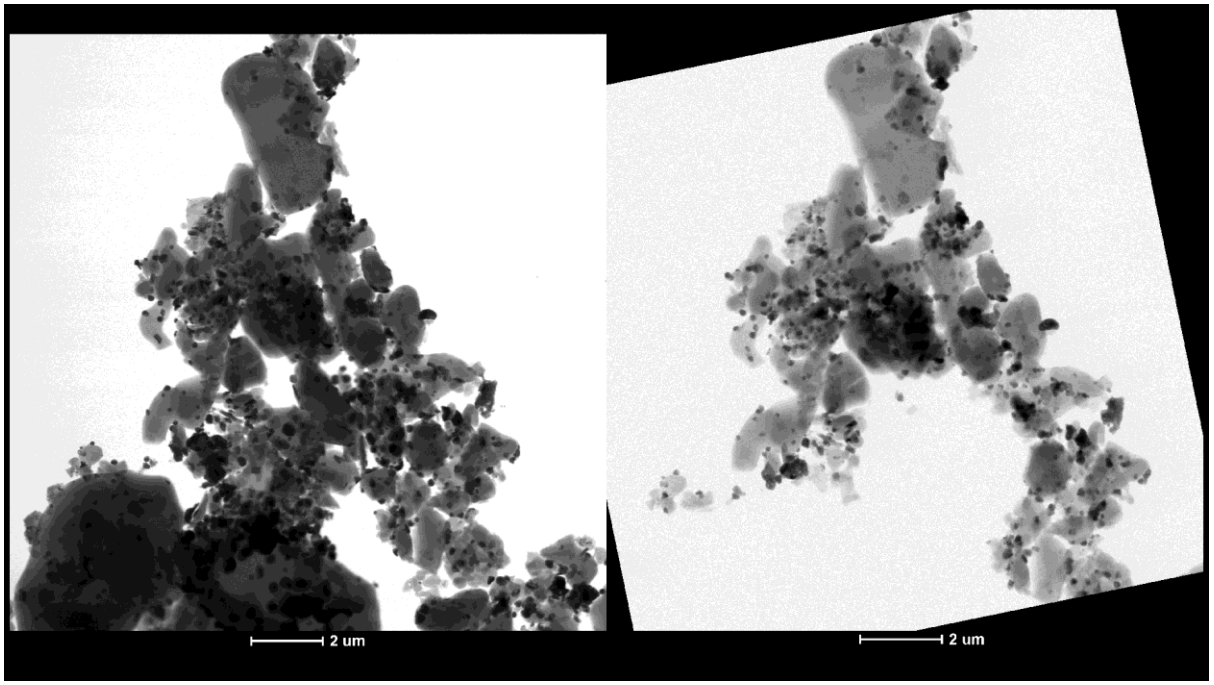

Figure 25. Mechanical breaking in wafer samples. Left 0h reaction, right 20h reaction.

Particle size changes

Silver particles can change in size due to a variety of mechanisms. For the classification of events the growth and decline in particle size will be followed. In Figure 26 an example of particle size decrease can be seen. In Figure 27 an example of particle size increase can be seen. Combination of multiple particles will only be logged as coalescence and not as particle growth. Minimal changes in particle size are hard to visually detect. Therefore it is possible for a certain area to have an increase in particle size without direct particle size events logged. Particle size increase can occur in combination with particle disappearance, which would be an indication of coalescence. Here it is

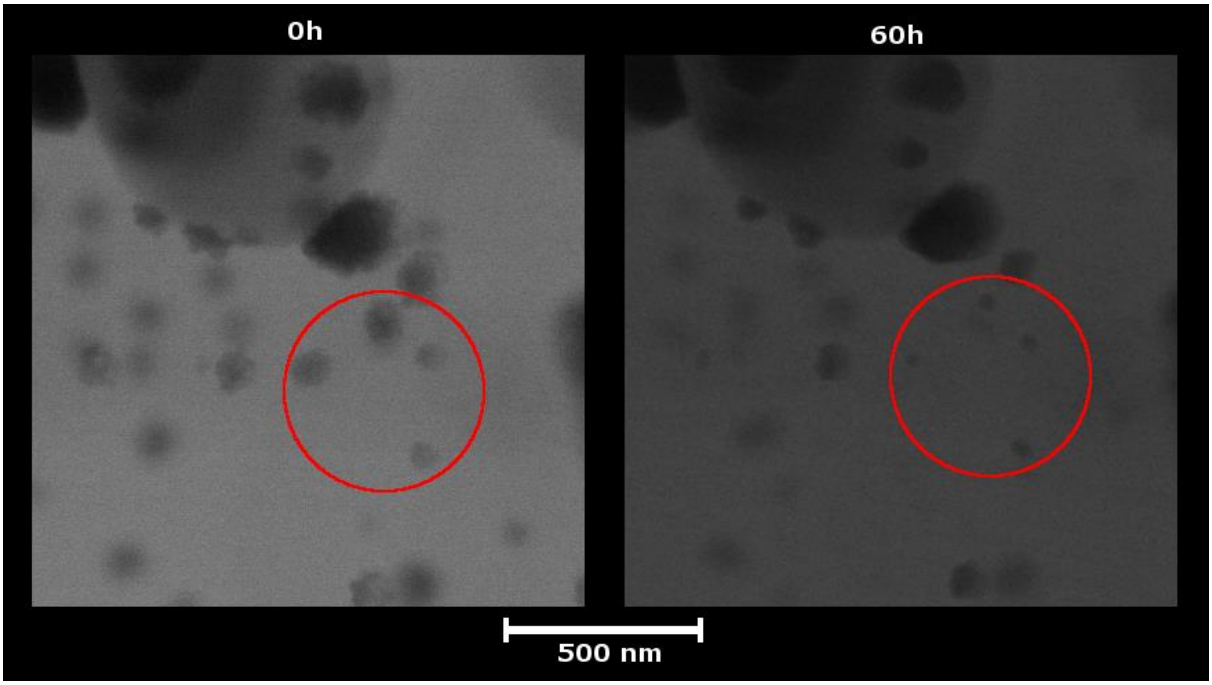

Figure 26. Example of particle size decrease, marked in red particles decreasing in size. Wafer = RP110-E.

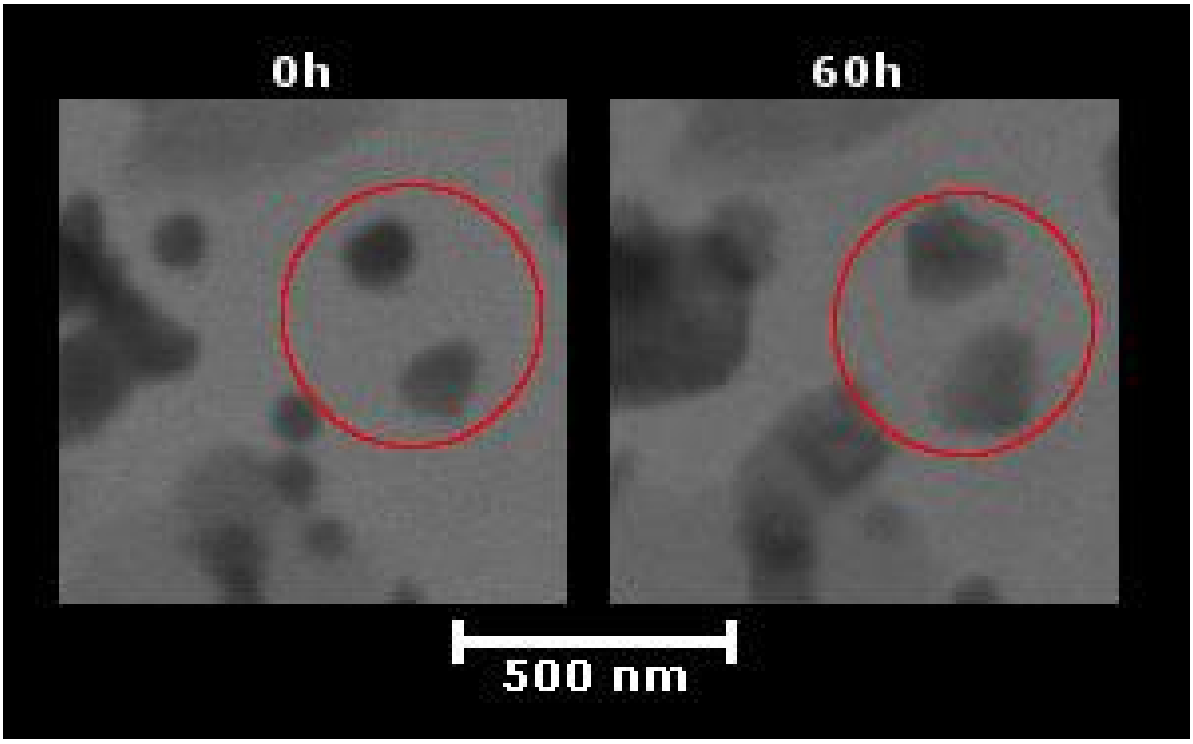

Figure 27. Example of particle size increase. Wafer = RP127-A.

assumed that a particle disappears and combines with a particle further away. Because two particles combine a change in particle size should be noticeable. If only disappearance is logged with an average increase in particle size, then this could be an indication of Ostwald ripening where small particles gradually lose their material and disappear. Their material will be evenly divided between multiple particles and it is less likely that a particle size increase event is detected.

Particle appearance/disappearance

Particles can appear and disappear for a variety of reasons. Several examples will be discussed here. The first is movement over relatively large distance. If a particle moves too far from its original position it is not possible to determine with certainty whether this particle is the same. Therefore this would be marked as one particle appearing and one particle disappearing. If all the events are summed and the amount of appearances and disappearances are roughly equal it can be concluded that this is because of movement over large distance.

The second possibility is the growth of particles that are initially too small to be measured. If a sample contains a number of small particles in the order of >5 nm, then it is possible that these particles are not detected on the first TEM image. On the subsequent image these particles could have combined or grown through another mechanism, making them large enough to be detected. In the final event count this would be characterized by a large number of particles appearing and an increase in total number of particles. The average particle size would likely decrease, however in this case it is better to look at the particle size distribution. It would be expected that the amount of small particles increases while the absolute amount of large particles does not increase.

The third option could be splitting of particles. If a large particle splits it creates two new particles of smaller diameter. This would be characterized by a decrease in overall particle size and an increase in number of particles counted. It would also be expected that a number of particle decrease events take place.

Surface wetting/particle reforming

In analyzing the TEM images the following could be observed. At 0 h silver nanoparticle would appear to be uniform and spherical. Starting at 20h and continuing on to 60 h and 60 h + 60 h VC, the particle would change in size and uniformity, see Figure 28. Its size would drastically increase, however the intensity of the increased area would go down. This decrease in intensity suggests either of two things: silver of lesser thickness or chemically different material with different density.

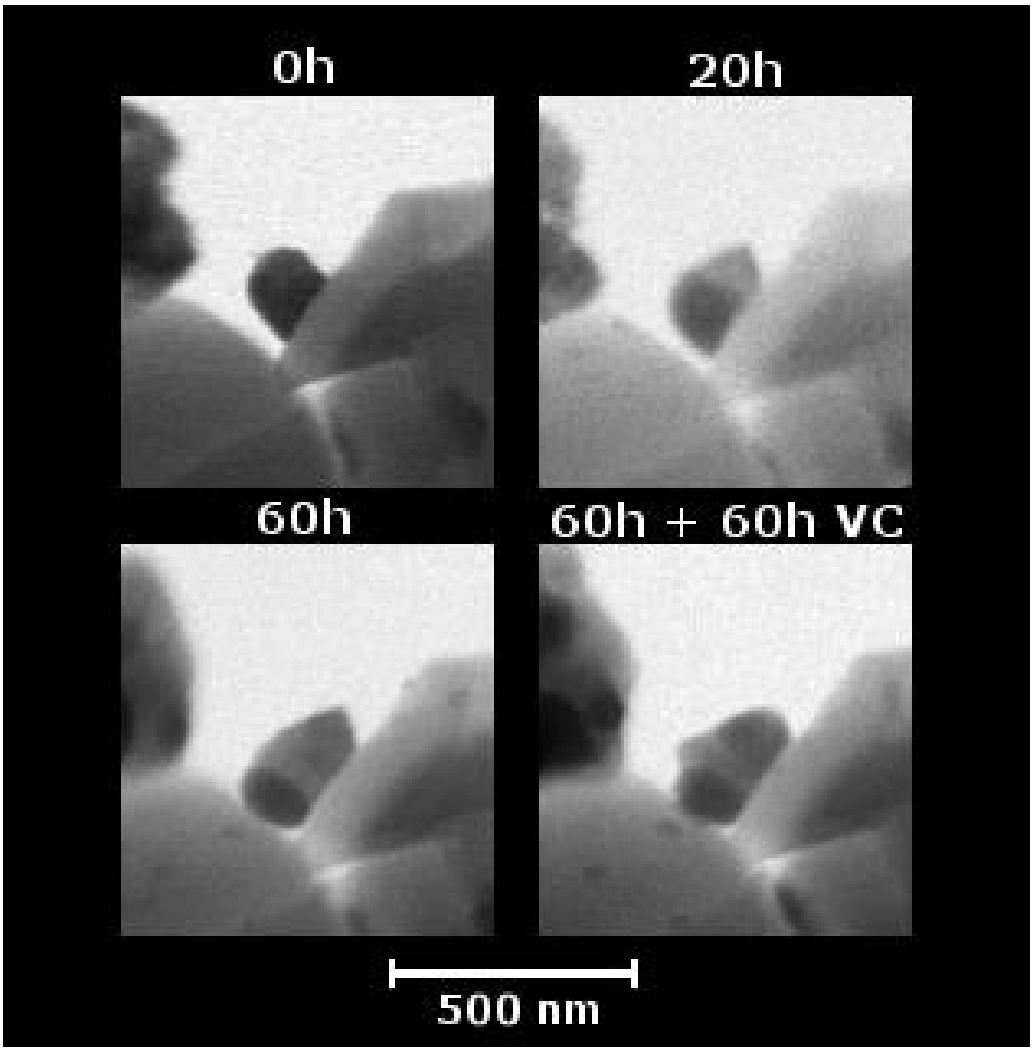

Figure 28. TEM image of a silver nanoparticle for 0, 20, 60 and 120h of reaction. The last 60h were carried out under atmosphere containing vinyl chloride.

For the creation of chemically different species two other molecules are available: oxygen and ethylene. The most obvious species that could form is silver oxide. Silver oxide has a lower density than silver (7.14 vs 10.49 g/cm^3 respectively) with the growth of the particle also making sense as the amount of mass doesn't change but its density gets lowered so its volume must increase. Still, it is unlikely that this is the case. Main reason being that silver oxides are unstable under illumination, therefore it is unlikely that they would remain stable under an electron beam. For the case of 60 h + 60 h VC another chemical is available, namely vinyl chloride. However it is unlikely that what is seen could be a chloride species. Since chloride is only available for the last transition, but no different phenomena form after this transition. It looks like a second darker area is formed at 60 h + 60 h VC, but the beginnings of this can already be seen in 60 h.

The most likely answer may lie in a physical difference of the nanoparticle. If it is assumed that both the light and dark part are metallic silver, than the logical conclusion is that the lighter area must be thinner. This means that during reaction, an initially spherical particle reforms into two phases. One particle phase which in location and thickness seems to resemble the original particle and a second phase that seems to spread outwards from the original particle in a much thinner particle. A process similar to this is wetting of a liquid on a solid surface. A schematic example of this process can be seen in Figure 29. This example shows a particle "A" with little wetting, while "S" has near perfect

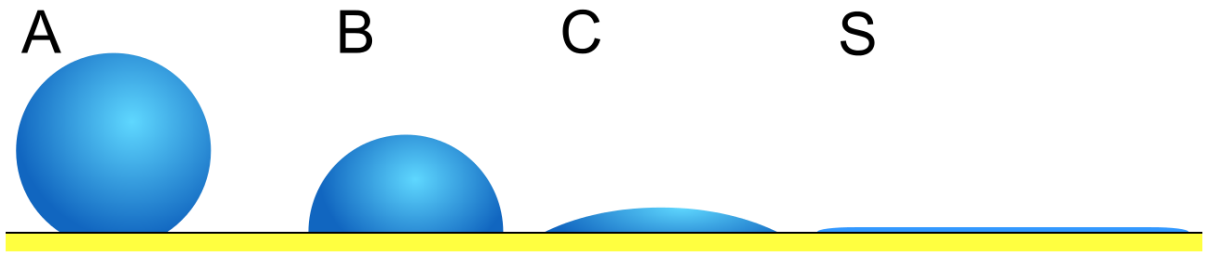

Figure 29. Example of surface wetting of liquid on a solid surface. A = non-wetting, S = perfect wetting.

wetting. Since the process in TEM looks similar to this process, it will be called wetting. Note that it is not assumed that this process is or is related to wetting, but only that it looks like it.

For the following analysis it is assumed that observed difference in Figure 28 is a physical one. In Figure 30 an analysis is made of the numerical grey value across a particle. This value fundamentally indicates the amount of electrons which are transmitted through the material. This value can also be

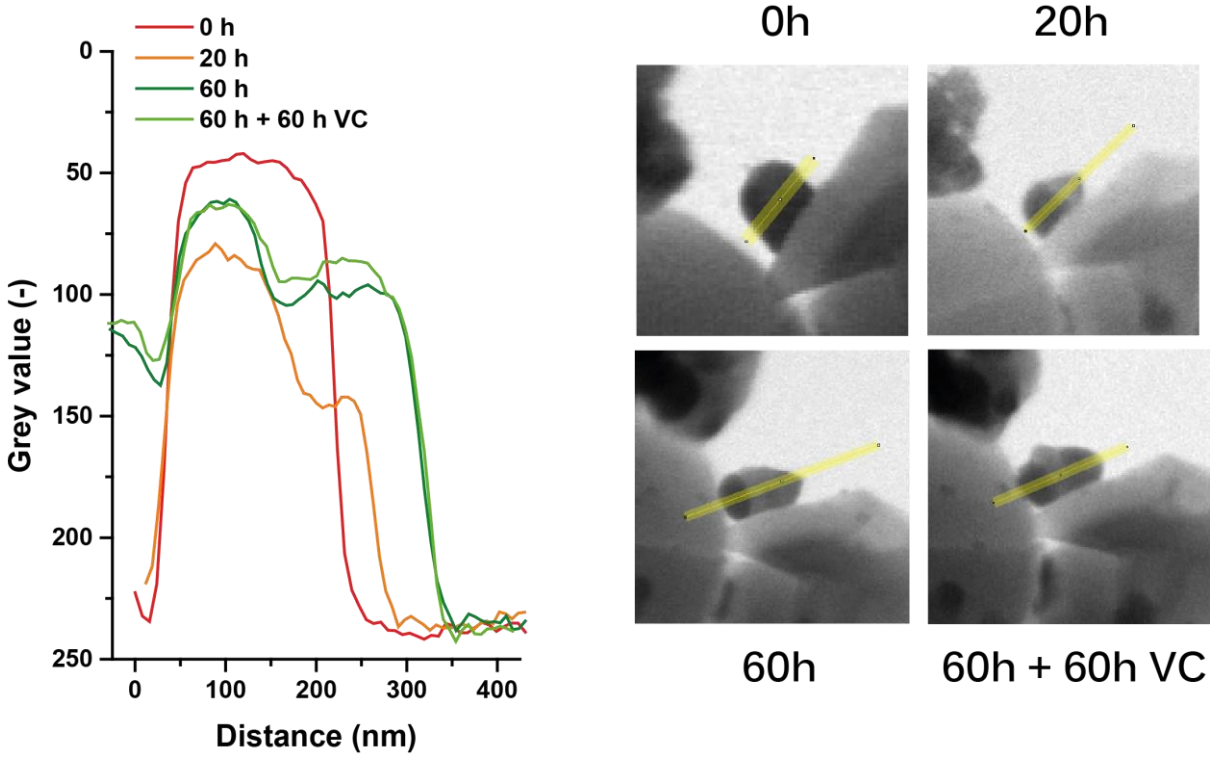

Figure 30. Left, grey value analysis of a particle. Right, path taken by analysis, all paths are taken left to right.

used to give an indication of the thickness of the material as function of the horizontal plane. In Figure 30 it can be seen that the particle starts of thick and decreases in thickness as function of reaction time. It also forms as second plateau to the right of significantly less thickness. This suggests that the material that is lost at the original position is being deposited to the right of the particle. It

can also be seen that a second increase in height takes places on the plateau. This could indicate a second particle growing next to the first particle connected through a lower area.

Figure 31 shows a representation of how wetting could take place on a silver particle during reaction. Figure 31a shows the situation before reaction and during pretreatment where particles are spherical. During the first 60 h of reaction in ethylene and oxygen (Figure 31b) the main particle shrinks in size and the material lost is deposited to the side in a lower plateau area. The start of a second particle can at this stage already be seen, see Figure 28 panel for 60 h. In Figure 31c, the reaction progresses and a chlorine moderator is added. The main particle decreases a bit further in size and the second particle is now clearly visible.

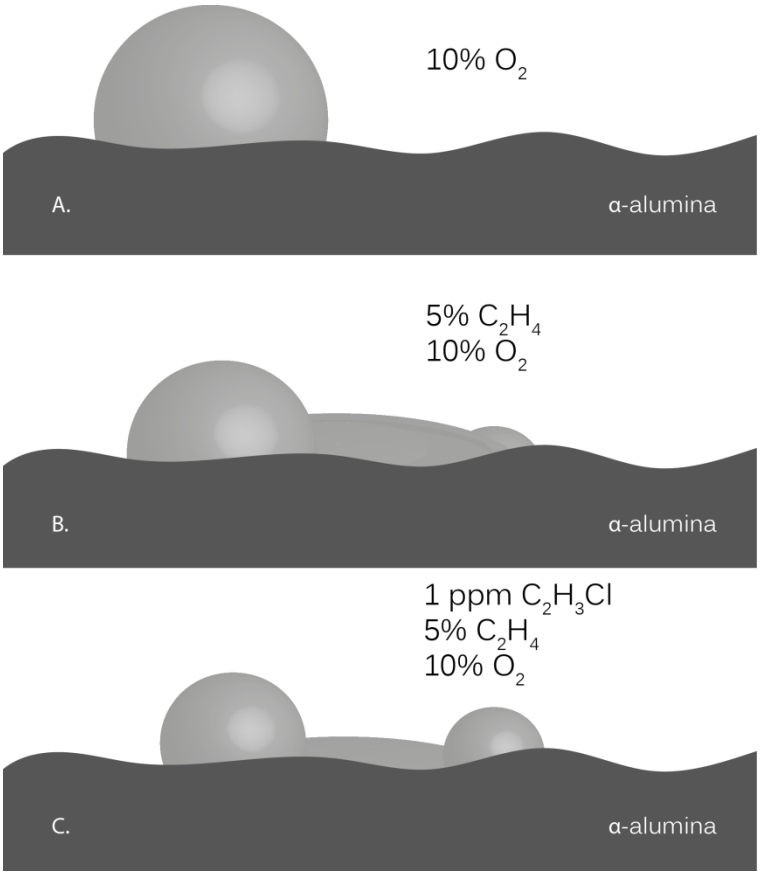

Figure 31. A 2D representation of a wetting silver particle during reaction

Pore formation

The formation of light spots on particles could be observed after reaction. It is known that pores can form in particles during reaction in processes like the Kirkendall effect [44]. This phenomenon could perhaps be related to this effect in some way. It is therefore thought that the epoxidation reaction contributes to the formation of these pores. An example of this pore formation can be seen in Figure 32. The pores are most visible after 120 h, but the beginning of them can already be seen after 20 h. It is also theorized that the pores form along the grain boundaries (explained in the results section "Monolayer oxygen equivalent") where the subsurface oxygen is present.

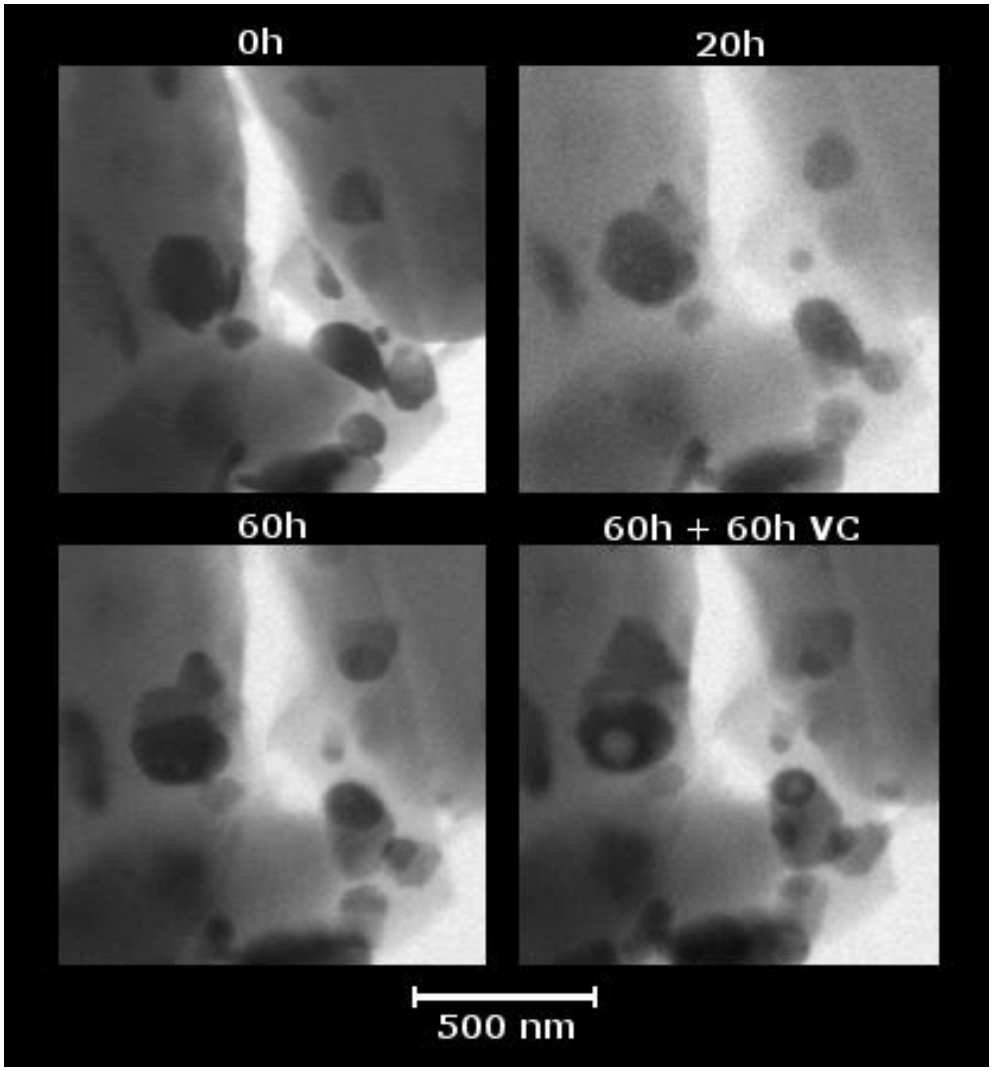

Figure 32. An example of pore formation during the epoxidation reaction.

Event Summary

Table 8 gives an overview of the selection criteria for each event as described in this section.

Table 8. Summary of events and their selection criteria.

Name	Selection criteria	Note
Pore formation	A lighter area formed on a particle	If one particle has more pores this will only be counted once
Coalescence	Two or more particles combine into one particle	If n particles combine into 1 particle this counts as n times coalescence
Wetting	Original particle decreases in size, a lighter area is formed attached to the darker area in a stain-like fashion	The method for particle size measurement of these wetting particles is described in more detail in appendix B.
Particle size increase	A clear increase in particle size	-
Particle size decrease	A clear decrease in particle size	-
Particle appearance	A particle appears in a location were previously there was no particle.	If it is clear a particle has moved no appearance or disappearance will be counted.
Particle disappearance	A particle disappears in a location were previously there was a particle.	If it is clear a particle has moved no appearance or disappearance will be counted.

Quantification

In order to do a more thorough investigation of the particle growth mechanisms of the silver supported particles a quantified analysis is carried out. The following procedures were used. First an area was found which had clear distinct particles and was in focus for all reaction stages. This area was marked and all events were indexed and counted. The selection of these events was done according to previously explained event characteristics. The particle sizes of all particles in the area were measured for images after 0 h, 60 h and 120 h of reaction. This information will be displayed in the next section. First each image will be discussed separately after which a more general analysis will follow.

The reaction 0 h → 60 h was carried out with a pre-treatment in 10% oxygen and 90% helium for 3 hours at 20 bar and 225 °C. After 3 hours the reaction mixture was switched to 10% oxygen and 5% ethylene in helium. For the transition 60 h → 120 h no pre-treatment was carried out. The samples were heated to 225 °C under 10% and 90% helium at 20 bar. When 225 °C was reached a switch was made to reaction gas with 1 ppm vinyl chloride, 10% oxygen and 5% ethylene in helium.

Large particle size wafers

The large particle size wafers are deposited with 10 wt% Ag/Al_2O_3 catalyst. This catalyst has also been used for a majority of pulse experiments. Previous particle size counts showed that this catalyst has an average particle size of 128 nm.

W3-Ag(128)-image-1

The first transition of this wafer is 60 hours under chlorine free reaction conditions, the results can be seen in Figure 33. This figure shows two graphs, on top an absolute particle size distribution with the particle sizes of all particles in the designated area. In the table the mean, number of particles and standard deviation is displayed. The second graph on the bottom displays the relative event data for the two transitions. In order to obtain the relative data, the events of a transition were divided by the total amount of particles at the end of the transition. So for the transition 0 h → 60 h, the amount of particles for the distribution for 60 hours was used.

For the first transition around 33% events as percentage of the total amount of particles were counted. Of these, particle disappearance was the major contributor with 12% of total or 16 particles absolute. For particles appearing and coalescence both 6 particles were logged, meaning that this would result in a net change of particles of zero. This means that the total disappearance of particles is 16 according to event data. From the particle size distribution count it can be calculated that 11 particles went missing during the transition. The 5 extra particles that should have gone missing might have been missed during the first count of particle sizes.

Table 9. Additional statistical parameters of W3-Ag(128)-image-1.

	Standard deviation [nm]	**Standard error**
0 h	59	4.88
60 h	65	5.89
120 h	51	3.5

In the table in Figure 33 it can be seen that the mean changes only 2 nm. In Table 9 the standard deviation and standard error of this value are given. Both of these values increase for the first transition. From this it can be concluded that the population contributing to the mean for 60 hours is more spread out than for 0 hours. In order to achieve the same mean with

equal amount of particles, more large and small particles need to be present. This suggests that Ostwald ripening is present for these particles, as this process causes the growth of larger particles at the expense of smaller particles, which would widen the distribution.

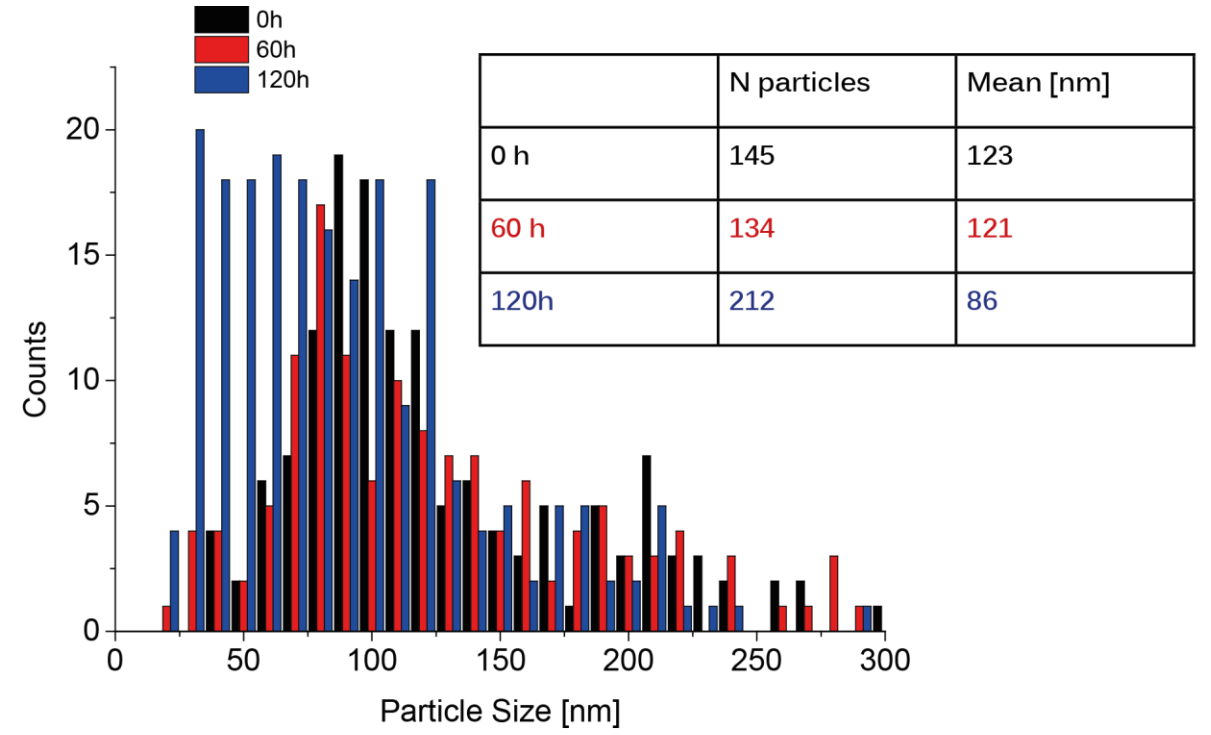

	N particles	Mean [nm]
0 h	145	123
60 h	134	121
120h	212	86

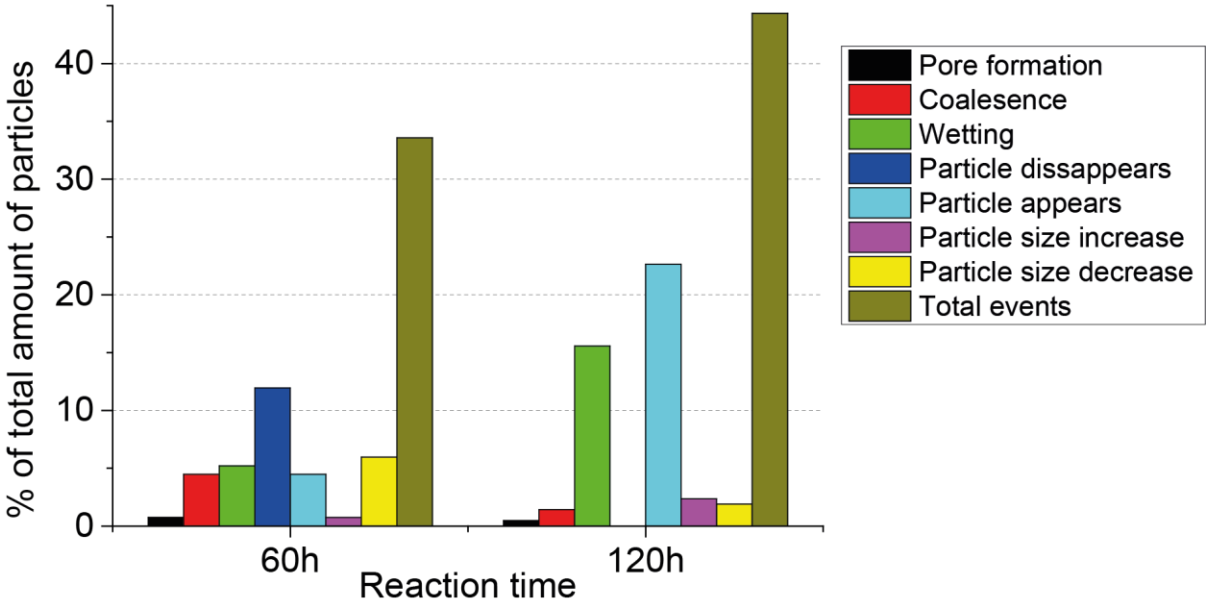

Figure 33. Particle size distribution and event data of RP103D-1A-10 image of W3-Ag(128)-image-1 wafer.

For the transition of 60 h to 120 h (Figure 33) a significant amount of small particles are formed, as can be seen in the particle size distribution. In the event log this can be seen as particles appearing. At the same time a substantial amount of wetting events can be observed. In order to exclude that the increase of small particles is due to coalescence of small non-visible particles the absolute amount particles was divided into three categories of small, medium and large particles, the results of which are displayed in Table 10. Since the amount of silver in this area should remain the same, because of conservation of mass. The silver for the increased amount of small particles should come

from somewhere. If the amount of medium and large particles stay the same, then it will be more likely that the small particles grew from non-visible. If the amount of large particles decreases and medium increases, then it means that the large particles shrunk and that their material was used for small particles.

In Table 10 it can be seen that for the transition 60 h → 120 h, the large fraction (150+ nm) the amount of particles decrease dramatically with a decrease of 12 particles leaving the category. At the same time the 100-150 nm category gains 18 particles. This in combination with the events of wetting and particles appearing means that the wetting process causes big particles to create small particles and shrink in the process. This information shows that the process of wetting can, under the right circumstances create separated small particles.

Table 10. Absolute count of different size fractions of RP103D-1A-10 image of W3-Ag(128)-image-1 wafer.

Category	Small than 100 nm	100 – 150 nm	Larger than 150 nm
0 h	50	57	38
60 h	55	42	37
120 h	127	60	25

W8-Ag(128)-image-1

In the first transition from 0 h to 60 h the major process taking place is wetting (Figure 34). At the same time the particle size increases and the total number of particles decreases. The process that was observed for wetting on W3-Ag(128)-image-1, of wetting creating smaller particles, is not observed here. Instead wetting increases average particle size. Note the increase of particle size is very dependent on how wetting events is measured as described in appendix B. In some cases it was observed that a wetting particle can merge with a particle that is close. This was not counted as an extra coalescence event. The number of particles that go missing in the particle count is 49, compared to 61 wetting events. This information combined mean that most of the particle decrease is caused by wetting. On the images this can be seen as wetting particles expanding and combining with neighboring particles. This effect makes wetting a very complex process. For the previous image the number of particles went up and particles size went down as a result of wetting, while for this image particle size went up and number of particles decreased.

During the second transition the particle size increases while the amount of particles remains the same. For events around 5% of wetting and 8% of particle size increase are recorded. The particle size increase in this area is quite substantial, especially in the range of 250 – 350 nm. The direct cause of this increase is not exactly clear from the event data. It is known however that the number of particles stays roughly the same for this transition, which could mean either of two things. A lot of material is transported from outside of the area and particles grow as a result of that. Alternatively, particles could get thinner through the process of wetting. In appendix B it is described how wetting particles are measured which could explain how the particle size can grow but how the number of particles can stay the same.

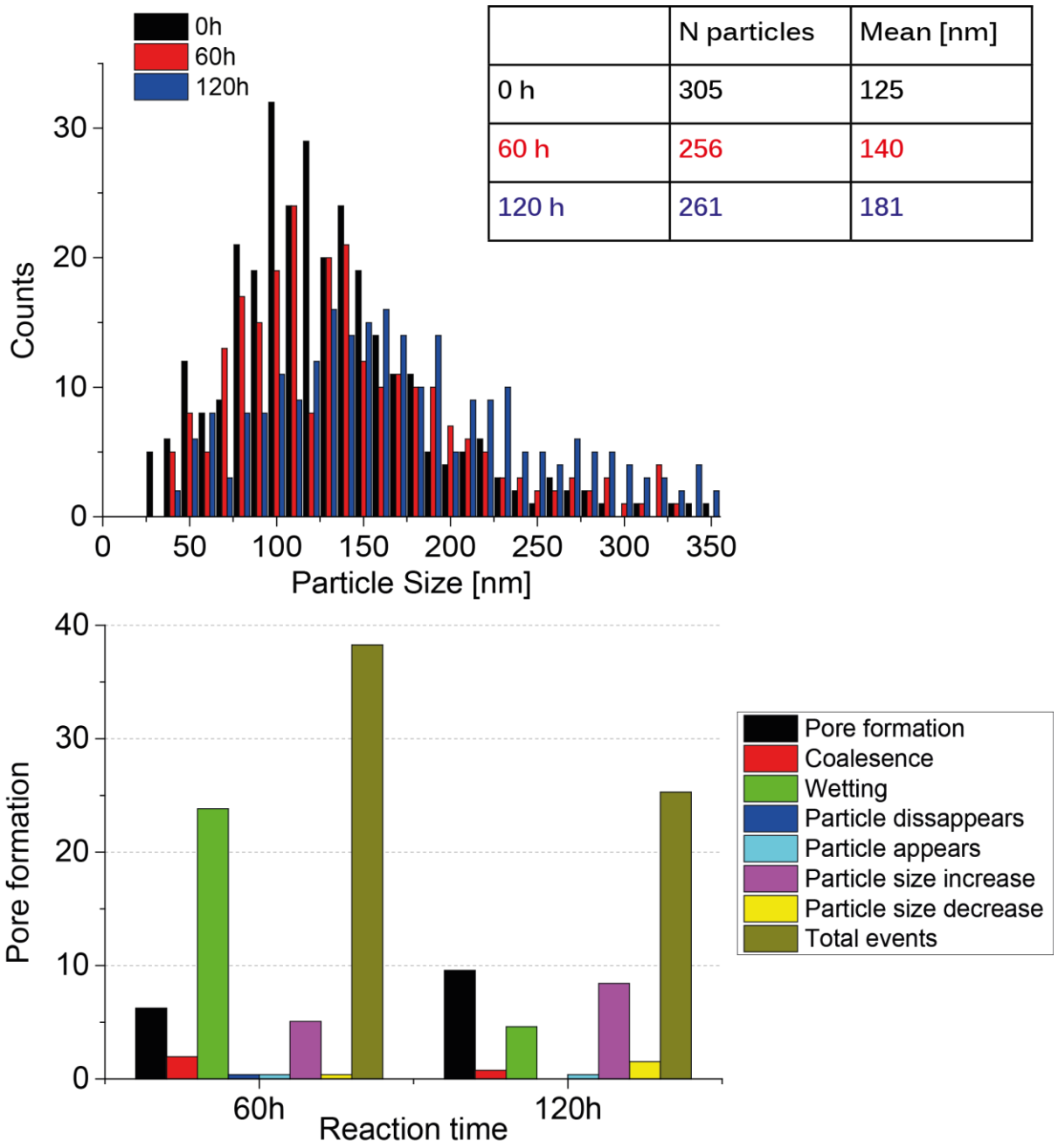

	N particles	Mean [nm]
0 h	305	125
60 h	256	140
120 h	261	181

Figure 34. Particle size distribution and events data of RP124N-1A-1 image of W3-Ag(128)-image-1 wafer.

Small particle size wafers

The smaller particles were created in the same way as the large particles, except the loading for this catalyst was five times lower at 2 wt%. The particles on this catalysts are on average much smaller and due to this a higher zoom level was needed when taking TEM images. Using a higher zoom level means more electrons per unit area which increased the likelihood of charging. As a result more areas are lost during measuring and smaller areas with fewer particles had to be used for counting.

W7-Ag(50)-image-1

In the first 60 h, the number of particles decreases and the particle size increases (Figure 35). Particularly a decrease of the smallest particles (<30 nm) can be observed in the particle size distribution. In the event data two main processes can be seen: coalescence and particle disappearance. It is clear that coalescence causes an increase in particle size and a decrease in number of particle size. However particle disappearance can be due to more than one cause. Both long distance coalescence and Ostwald ripening could cause a number of particle disappearance events. Both mechanisms would also cause a decrease in the number of particles.

Table 11. Absolute event data W7-ag(50)-image-1.

Event	Counts
Coalescence	9
Particle disappearance	11
Particle appearance	1
Particle size increase	3

In order to determine which mechanism is present the absolute event data will be used as displayed in Table 11. From the particle count in Figure 35, it is known that during the first transition 40 particles go missing. 9 of these will have gone missing due to coalescence if it is assumed that 2 particles form 1 coalescence event. A net amount of 10 particles disappearance events were logged together with 3 particles size increase events. If long distance coalescence occurs, it would be likely that the final particle has a significant increase in size and would be detected as particle size increase. It is therefore assumed that of the 10 disappearance events, 3 were due to coalescence. The remaining 7 would have been due to Ostwald ripening.

Of original 40 missing particles, 9+3 went missing due to coalescence and 7 went missing due to Ostwald ripening. Here it becomes clear that logging events does not completely cover all particles, as for half of the particles it is not clear which mechanism is responsible. For the particles that were logged, the leading mechanism is coalescence with around double the amount of particles missing as for Ostwald ripening.

The transition of 60 h to 120 h seems to have little effect on any value. The changes that do occur could be due to measuring inaccuracy or some exchange of silver atoms between particles. Another area on the same wafer (see next section ''W7-Ag(50)-image-2'') does exhibit more events, however this area only had a small amount of particles and therefore this need not be representative.

The lack of change during the chlorine reaction could be due to the sequence of experiments. First 60 h of chlorine-free reaction mixture was used. For the subsequent 60 h reaction, chlorine was used. This does not mean that the chlorine causes the lower amount of events. It could be the case that the small particles react quickly and reach a relatively stable state in 60 hours. In subsequent experiments nothing would change regardless of chlorine addition.

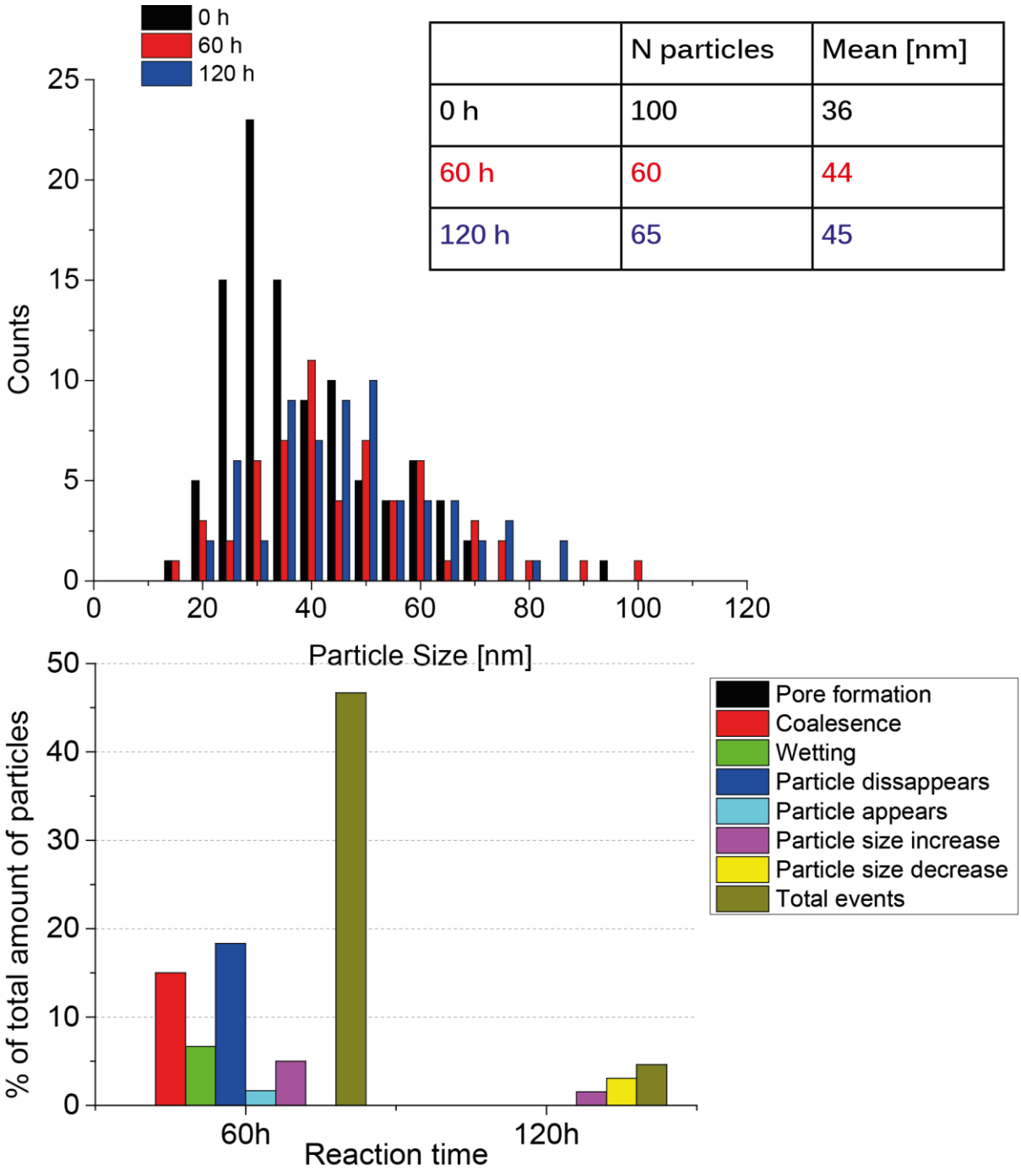

	N particles	Mean [nm]
0 h	100	36
60 h	60	44
120 h	65	45

Figure 35. Particle size distribution and events data of RP110E-1C-2 image of W7-Ag(50)-image-1 wafer.

W7-Ag(50)-image-2

This is only a small area with particles located on an isolated support particle (Figure 36). During the first 60 hours the biggest change in particle size distribution can be observed. This is probably due to the event of particles disappearing. However the event particle size increase was not directly measured. This could be due to the particle size change not being visible due to the slight change for small particles. If this is the case it is likely that the growth mechanism used is Ostwald ripening, as for coalescence it would be expected to see clear particles size increases due to two particles completely combining their material. For Ostwald ripening it is logical that the material of one particle disappearing would be spread out over multiple particles and therefore a direct particle size increase would not be detected. Therefore the leading mechanism in this image seems to be Ostwald ripening.

For the second transition the particle size increased 5 nm due to one coalescence and one wetting event. One particle moves its position which is indicated by an appearance disappearance combination. One particle disappears completely, which is due most likely due to Ostwald ripening since there is no direct particle size increase observed.

A general conclusion that can be drawn from the small particle system is that most of the particle size changes happen in the first 60 hours. This would also be expected due to the classical mechanisms of coalescence and Ostwald ripening. For coalescence, smaller particles are more mobile and therefore they can combine quicker as shown by Thomas Hansen *et al.*[36]. For Ostwald ripening smaller particles mean relatively more particles are corner, edge or surface atoms compared to larger particles. Therefore they are less stable and the driving force for Ostwald ripening would be on average bigger than for larger particles.

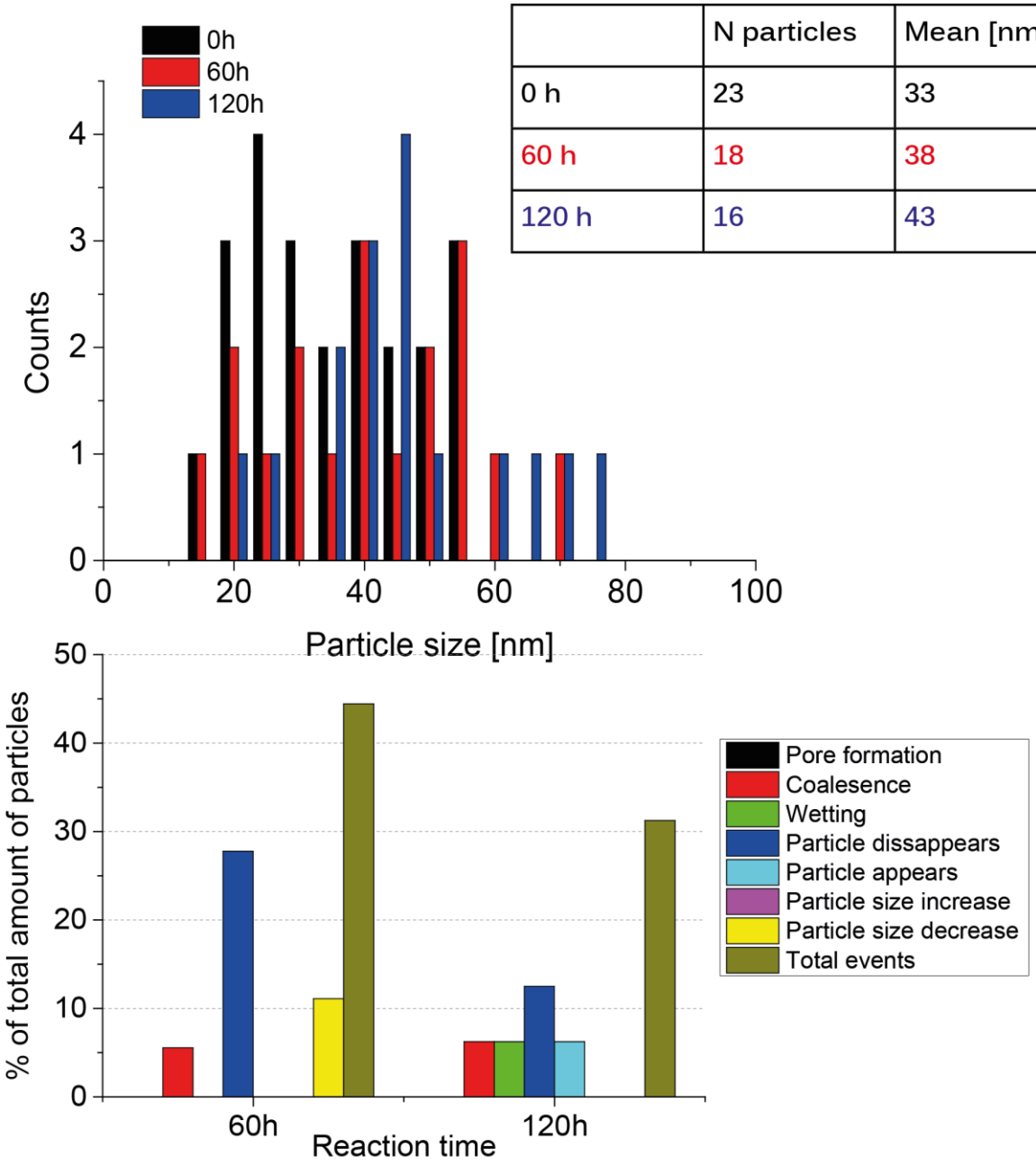

	N particles	Mean [nm]
0 h	23	33
60 h	18	38
120 h	16	43

Figure 36. Particle size distribution and events data of RP110E-2B-2 image of W7-Ag(50)-image-2 wafer.

Cesium promoted particle wafers

The following samples consisted of the base 10 wt% silver catalyst on α-alumina, cesium was added simultaneously during the synthesis of silver and a promotion of 750 ppm cesium was reached [31].

W9-Ag(110)/Cs-image-1

During the first 60 hours (Figure 38) a lot of change in the particle size distribution can be observed. This image in particular has the highest occurrence of events of all at 70%. It must be noted that this 70% was calculated based on the amount of particles at 60 hours. Several events are a major contributor. The first is coalescence of particles. The second with a roughly equal amount of events is wetting. It was observed that wetting particles could combine with neighboring particles due to proximity. These two processes both increase particle size and decrease particle amount. Two secondary events with around 9-10% of particles are particle disappearance and particle size increase. It is very likely that these events combined are coalescence events, but due to the distance between particles it was not initially recognized as coalescence. This would bring the actual amount of coalescence events up to 30%.

Wetting in this particular sample was very severe and 1 wetting event could merge with 2-5 particles due to close proximity. An example of this is given in Figure 37. Therefore it is not possible to determine to what extend Ostwald ripening was present with this analysis.

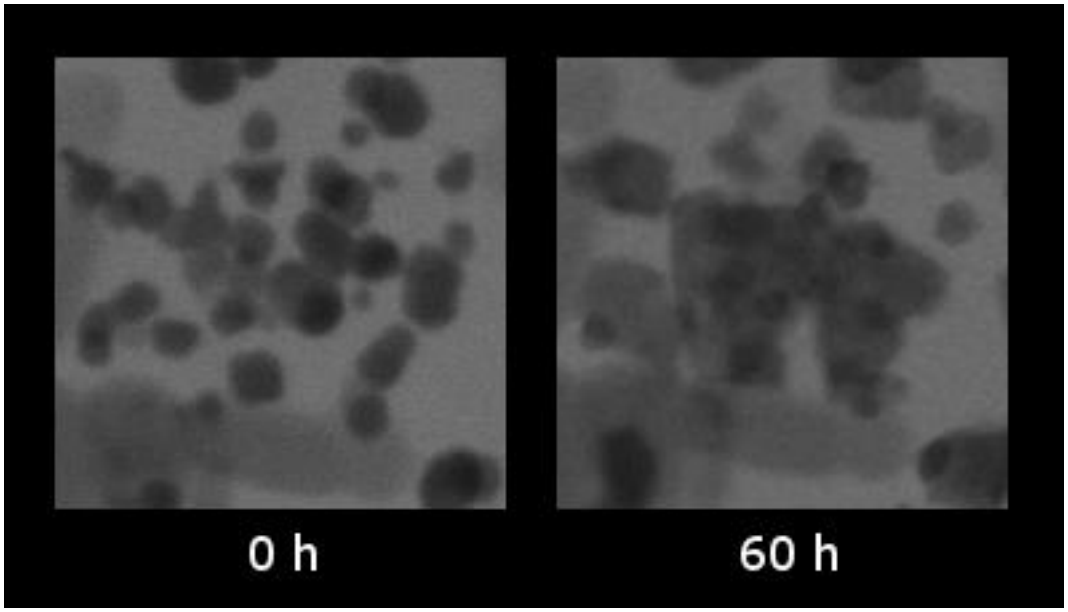

Figure 37. An example of wetting combining with multiple particles in the area. Sample = 127A-1A-4.

For the second transition the main event that takes place is the formation of pores. All other events are only present in minimal to no quantity. Particle size decreases by 7 nm and number of particle is 5% lower, but this is not significant enough to indicate real change. The particle size distribution for this transition also stays roughly the same.

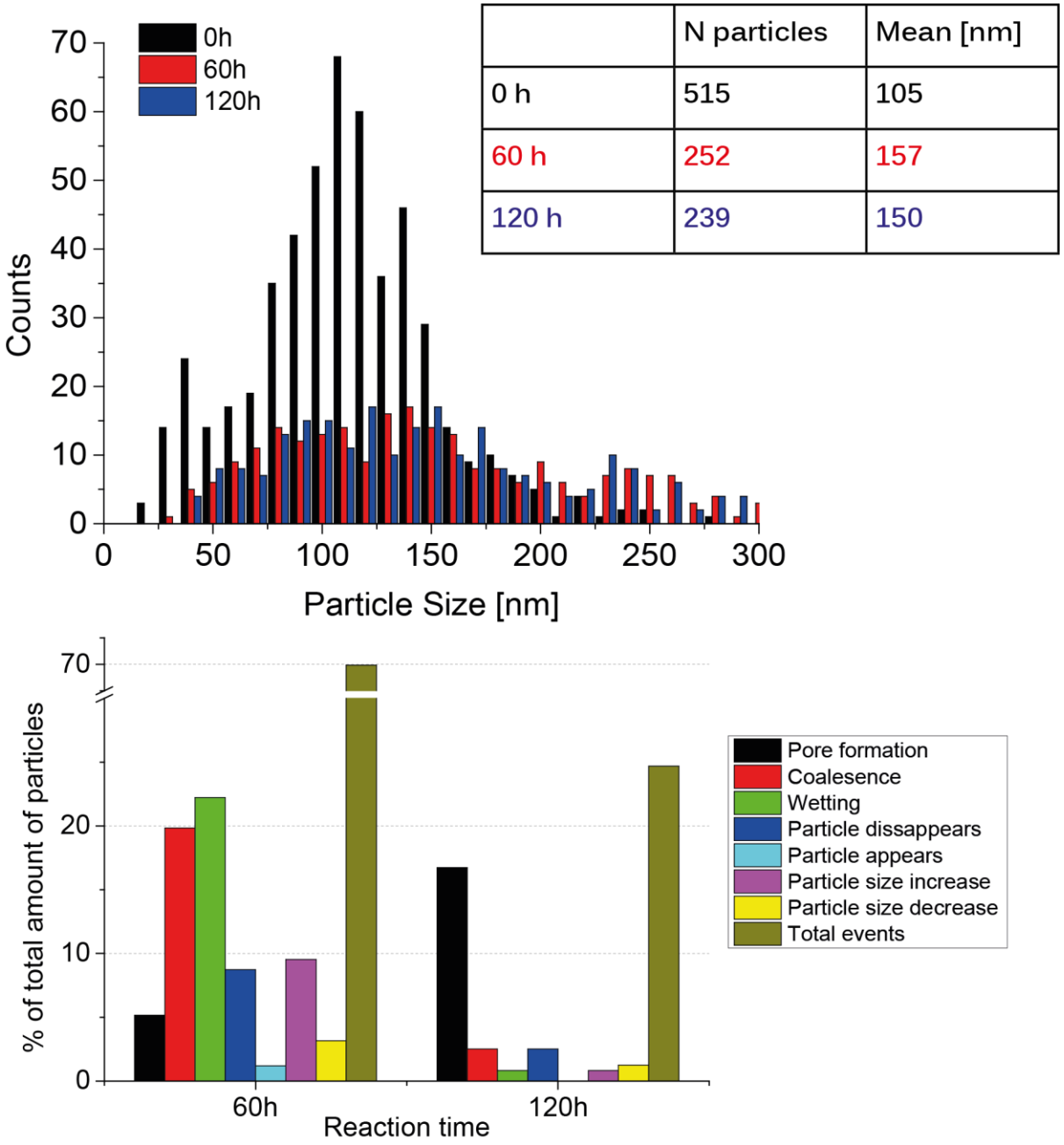

	N particles	Mean [nm]
0 h	515	105
60 h	252	157
120 h	239	150

Figure 38. Particle size distribution and events data of RP127A-1A-4 image of W9-Ag(110)/Cs-image-1 wafer.

W9-Ag(110)/Cs-image-2

For the first 60 h (Figure 39) the main process is coalescence, as can be seen in the event data. It can also be seen in the particle size distribution, where initially large quantities of small particles are converted to a smaller amount of large particles. Wetting also plays a significant role and might be in part responsible for the creation of some of the larger particles.

During the second transition the amount of events is very low, this can also be seen in the particle amount and size distribution which both show little change. This same absence of events can also be observed with the previous cesium sample (W9-Ag(110)/Cs-image-2).

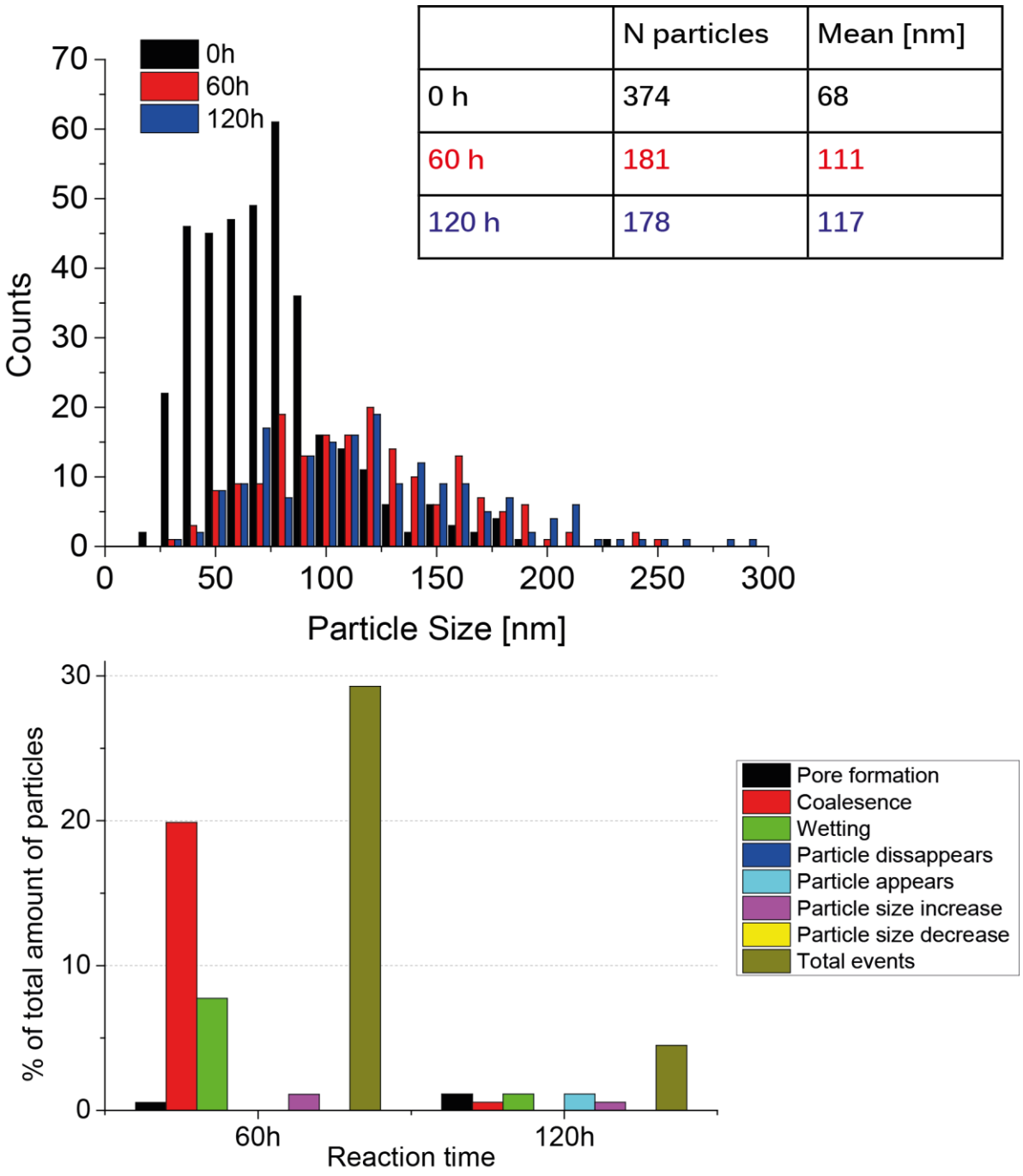

	N particles	Mean [nm]
0 h	374	68
60 h	181	111
120 h	178	117

Figure 39. Particle size distribution and events data of RP127B-3C-1 image of W9-Ag(110)/Cs-image-2 wafer.

General Wafer discussion

Pore formation is a relatively minor process in all of the samples, with usually 1-10% of particles affected. However, pores are only marked if they are clearly visible on the particles. It is possible that the total amount of particles that have pore formation is higher, but that their pores are too small to detect. No pore formation events were found for the small particle sizes. This could be due to no pores forming or again due to them being too small to detect. No pores forming for the small particles could be due to their size. For small particles it was measured that no subsurface oxygen was present and that the grain boundaries associated with this were also not present. It is theorized that pores form along grain boundaries, perhaps as a result of the interaction with subsurface oxygen. The fact that small particles have no subsurface oxygen or pores would support this argument. Pore formation for the large and the cesium particles seems to be almost the same for both the first 60 h and the second 60 h. From this it can be concluded that the addition of chlorine does not seems to have an effect on the amount of pores forming. Cesium promotion also does not seem to have a significant influence on the occurrence of pores.

For large particles coalescence is a relatively minor process with around 2-5% of particles being affected, see Figure 40. Cesium promoted particles however have 20% of particles affected by coalescence during the first 60 hours. This suggests that cesium promotion in the absence of chlorine would increase the number of coalescence events. However more particles and images would have to be analyzed to give a more definitive answer of this effect. A probable cause for the higher amount of coalescence events is the difference in initial particle size distribution as can be seen in Figure 39. Here it can be seen that the cesium promoted sample starts with a substantial amount of particles of size 20 – 80 nm. After 60 hours of reaction these particles are gone due to coalescence. In order to exclude this effect other areas could be analyzed and systems with similar particle size distributions could be compared to each other.

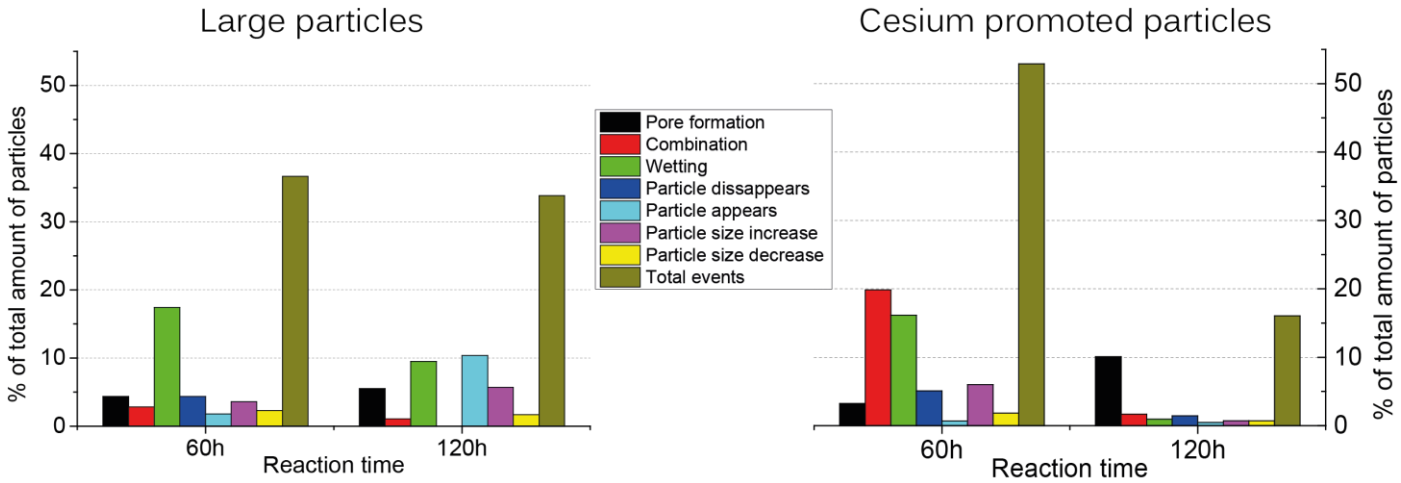

Figure 40. Cumulative amount of events for large and cesium promoted particles. Absolute data can be found in table 12

For the cesium promoted samples, if chlorine is added, the amount of change in particle size distribution decreases and the amount of non-pore formation events is low compared to the initial 60 h of reaction, see Figure 40 and Figure 41. For unpromoted large particles this decrease in change is not detected. Activity tests done on this particular catalyst show that cesium promotion is beneficial with respect to activity and selectivity in the case that chlorine is added[31]. This could

mean that the simultaneous addition of chlorine and cesium have a stabilizing effect on particle growth processes, which manifests itself in better catalytic performance.

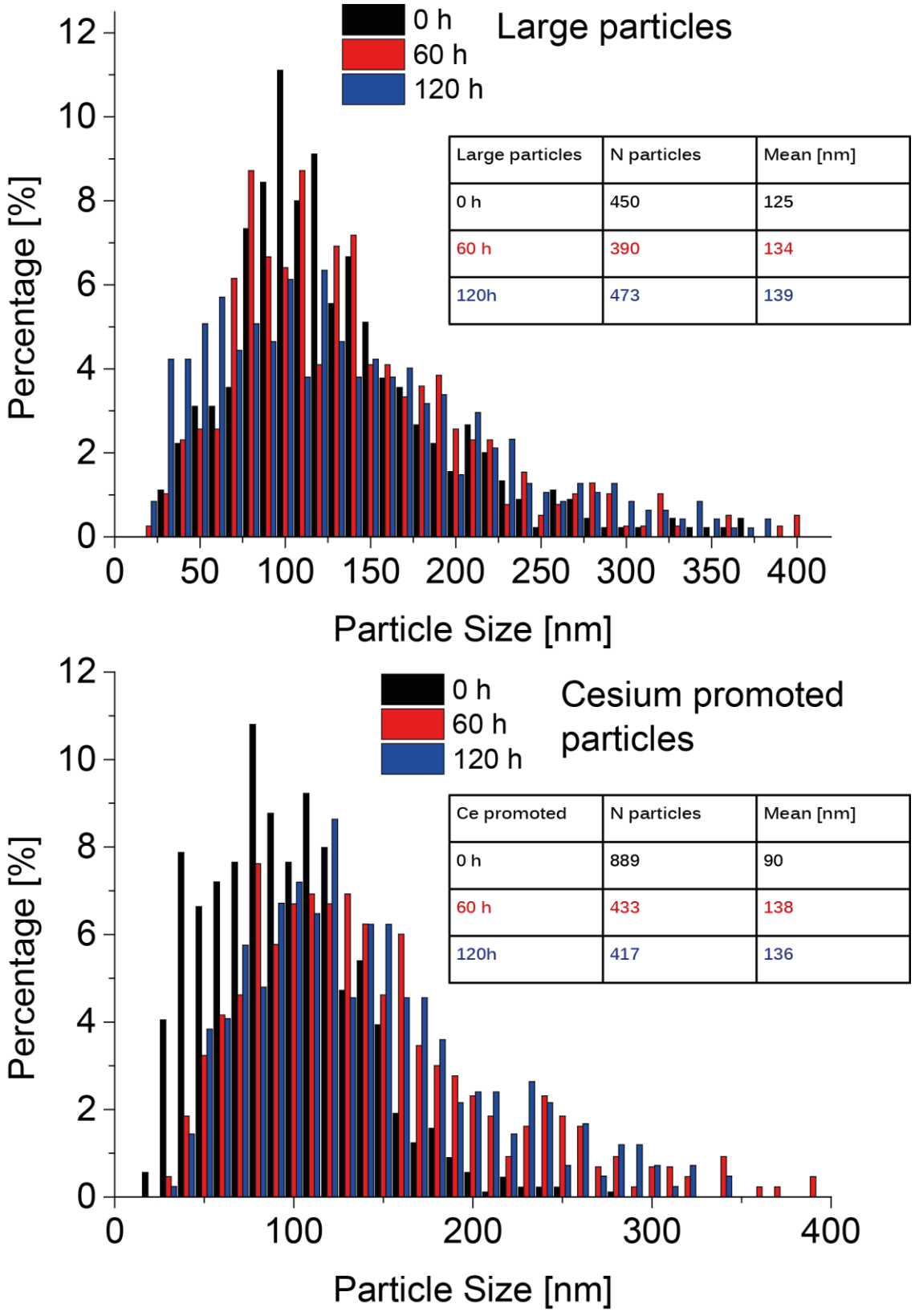

Large particles	N particles	Mean [nm]
0 h	450	125
60 h	390	134
120h	473	139

Ce promoted	N particles	Mean [nm]
0 h	889	90
60 h	433	138
120h	417	136

Figure 41. Relative particle size distributions for the total of large and cesium particles.

Wetting is an interesting process in that its behavior is unlike other classic sintering mechanisms like coalescence or Ostwald ripening. Coalescence relies on the mobility of particles and Ostwald ripening on the relative stability of surface vs bulk atoms. The behavior of wetting seems to resemble a fluid system where the interaction between fluid-solid and fluid-fluid is determining for the shape of particles. In such system the driving force is the surface tension between the 3 phases. From the given data it is not possible to conclude which aspect of the reaction causes this wetting to occur.

Table 12. Absolute event data for the total amount of large and cesium promoted particles.

Sample	**Events 0-60 h**	**Events 60-120h**
Large particles	98	66
Cesium promoted particles	53	8

Wetting affects around 15% of large and cesium promoted particles during the first 60 h of reaction and the large particles in the second 60 h. This makes it a quite significant process concerning particle growth. For the first wafer W3-Ag(128)-image-1 wetting caused a number of small particles to break off and lowered overall particle size. For wafer W8-Ag(128)-image-1 the complete reverse was observed. Here particles were swallowed by a wetting particle and average particle size increased. However it should be noted that the effect of wetting on the particle size might have been counted inaccurately and therefore it is unclear what the precise effect is on particle size. Details about this can be found in appendix B. Statistically it is difficult to give conclusive evidence about the effect of wetting.

Conclusions wafers

Using Si_3N_4 wafers it is possible to follow particle growth at a very detailed level during reaction at industrial conditions. In this thesis an approach was developed on how to prepare wafers with deposits of supported catalysts. Indexed TEM images were compared and clear differences could be observed between particles. A method for the analysis of the TEM data was explored and some conclusions could be drawn from this.

During the first 60 hours of reaction a number of processes could be observed. Two classical processes namely: coalescence and Ostwald ripening are present in the same order of magnitude. It is however not possible to determine whether one process is more prevalent. A third process, which was named wetting, was observed. This process was analyzed and it was determined that it looks like classical liquid wetting. From statistical data it was found to occur for around 15% of all particles making this a quite significant process of particle growth. How the wetting process affects the particle size and particle size distribution could not be determined and requires more thorough investigation.

The formation of pores in particles could also be observed. It was determined that these pores only form under reaction conditions. Pore formation is a process that affects a relatively small amount of particles (1-10%) in 120 hours of reaction. It seems to be unaffected by chlorine addition or cesium promotion. No pore formation was observed for small particles, which is likely due to the fact that small particles do not have grain boundaries or amount of subsurface oxygen to facilitate pore growth.

When chlorine was introduced to the reaction the results for large particles were minimal. Small particles seemed to have less particle size change during the chlorine reaction, but not enough of these particles were analyzed to give a definitive answer. Promotion with cesium showed an increase in the amount of coalescence events as compared with large particles. However it was determined that this was not caused by cesium, but rather was a result of a different particle size distribution between the large and cesium promoted catalysts.

The combination of cesium promotion and chlorine moderation yielded interesting results. It seemed to stabilize the particle growth on the catalyst and caused minimal changes in particle size distribution. As enough particles of these samples were analyzed it can be concluded that these results are valid. It is very possible that the stabilization of particle growth is caused by cesium promotion which produces improved catalytic performance on the catalysts.

Recommendations

While using TPD profiles to follow oxygen coverage, spectroscopic methods like Raman spectroscopy would make it possible to more accurately follow the oxygen coverage during a pulse experiment. It is recommended to use a more sensitive setup in order to minimize silver exposure to light, while maximizing Raman signal.

Oxygen pulse experiments could be expanded for other technical catalysts. Special interest would be for a gold doped catalyst without possible chlorine poisoning. Also the addition of vinyl chloride as promotor would be interesting to follow for the unpromoted and copper catalyst. Although it should be noted that a very sensitive setup is needed since conversion will be lower.

The wafer experiments have created a lot of interesting data, however due to time constraints not all of it has been analyzed to its full potential. The best approach for analyzing this data would be to automate it, but it is unknown if current software programs are capable of analyzing such images. It would therefore be recommended to try and develop software which would make automatic data processing possible. This would allow more data to be processed and make the quantitative analysis more accurate. If further analysis were to be undertaken, it might be useful to re-evaluate whether more events should be added. It is also mentioned in appendix B, that the method for the measurement of wetting particles should be adapted. For the event count of coalescence it would also be better to count both the amount of particles before and after coalescence. The current method only always counts a coalescence event as 1, however it is possible for 3 or more particles to combine into 1 particle and this can and should be taken into account.

It was shown that the wetting process affects quite a large number of particles. It would therefore be interesting to investigate what the mechanism behind this process is. If it is indeed connected to classic liquid wetting and surface energies, then it might be useful to carry out this experiment at lower or higher pressure, since at different pressure surface energies will vary. Or alternatively, another support could be used to so if the same process is repeated there.

The method for following particle size growth used in this thesis could be used for other catalytic systems. Especially systems that have large (diameter 50+ nm) particles would be suitable for this. Smaller particles could also be used, but higher magnifications and resolutions are required which increases the risk of charging. To reduce the risk of charging another wafer material might help. For example some non-oxidation catalyst metal like aluminum would be suitable.

Acknowledgement

I am very happy with the completion of my master thesis. It has been a long road with its ups and downs, but I would not trade it in for the world. I would now like to take the opportunity to thank the people whom without this project would not have been possible.

I would like to thank Professor Emiel Hensen for the opportunity to do my graduation project in his group. I am especially grateful for the many the opportunities that he has given me, like going to NCCC and his help in finding an internship at BASF. I also would like to thank Dr. Heiner Friedrich for his valuable input for this project and with the analysis of the data.

I especially would like to thank Arno van Hoof for is supervision during my project. The many talks and discussions about my experiments helped me to think about the problems and you made me figure things out for myself first before you gave me your answer. He really helped me become a better chemist and researcher and for this I am very grateful.

I would like to thank Eline Hermans and Shreyas Amin for the use of their catalysts and catalyst synthesis procedures; they work perfectly and were of high quality. Many thanks to Shreyas in particular for showing me the synthesis procedures and for his help in using the pulse setup.

Спасибо to dr. Nikolay Kosinov for his insight and help during my project. I would like to thank him for the opportunity to join him on the beam trip to Grenoble, I learned a lot from this and really enjoyed my time there.

Verder zou ik graag mijn ouders en zusje bedanken voor hun hulp en steun tijdens dit project en ook mijn hele studie. Het is fijn om te weten dat ik altijd naar huis kan komen voor de rust en stilte van Schinnen.

Mijn medestudenten op kantoor wil ik bedanken voor een mooie tijd en genoeg afleiding tijdens de lange dagen van verslag schrijven. In het bijzonder Rudie voor de talloze discussies over ons onderzoek. Deze hebben mij geholpen om zaken soms van een andere kant te belichten of om nog beter over zaken na te denken.

Lastly I would like to thank everybody from the IMC group for their hospitality and for their contributions to my project. It really was a wonderful time for me.

References

[1] T. B. Journals, “Ethylene Oxide Market Global Key Producers, Chain, Size, Consumption, Upstream, Downstream and Growth Rate 2.0% in 2017-2021,” 2017. [Online]. Available: https://www.bizjournals.com/prnewswire/press_releases/2017/07/17/enUK201707178573. [Accessed: 16-May-2018].

[2] P. Newswire, “Global and China Ethylene Oxide (EO) Industry Report, 2017-2021,” 2017. [Online]. Available: https://www.prnewswire.com/news-releases/global-and-china-ethylene-oxide-eo-industry-report-2017-2021-300493113.html. [Accessed: 16-May-2018].

[3] CRI Catalysts, “Omega and Ethylene Oxide / Ethylene Glycol Technology,” 2017. [Online]. Available: http://www.shell.com/business-customers/chemicals/factsheets-speeches-and-articles/factsheets/omega.html. [Accessed: 16-May-2018].

[4] P. K. Banerjee, “Silver, Silver Compounds, and Silver Alloys,” *Ullmann’s Encycl. Ind. Chem.*, vol. 33, no. 1, 2012.

[5] J. J. Becher, *Physica subterranea*. Leipzig: Officina Weidmanniana, 1669.

[6] J. Galil, “An ancient technique for ripening sycomore fruit in East-Mediterranean Countries,” *Econ. Bot.*, vol. 22, no. 2, pp. 178–190, 1968.

[7] S. Rebsdat and D. Mayer, “Ethylene Glycol,” *Ullmann’s Encycl. Ind. Chem.*, pp. 547–572, 2012.

[8] Union Carbide, “Chapter Two PETROCHEMICAL PIONEER (1920-1940),” 1940.

[9] L. Petrov, A. Eliyas, and D. Shopov, “A kinetic model of steady state ethylene epoxidation over a supported silver catalyst,” *Appl. Catal.*, vol. 18, no. 1, pp. 87–103, 1985.

[10] P. Lahtinen, E. Lankinen, M. Leskelä, and T. Repo, “Insight into copper oxidation catalysts: Kinetics, catalytic active species and their deactivation,” *Appl. Catal. A Gen.*, vol. 295, no. 2, pp. 177–184, 2005.

[11] M. O. Ozbek, I. Onal, and R. A. Van Santen, “Why silver is the unique catalyst for ethylene epoxidation,” *J. Catal.*, vol. 284, no. 2, pp. 230–235, 2011.

[12] R. A. Van Santen, “The Mechanism of Ethylene Epoxidation Catalysis,” pp. 131–141, 2013.

[13] Shell, “Ethylene oxide/Ethylene Glycol (EO/EG) Processes.” [Online]. Available: http://www.shell.com/business-customers/global-solutions/petrochemicals-technologies-licensing/ethylene-oxide-ethylene-glycol-processes.html. [Accessed: 21-Nov-2017].

[14] J. K. Lee, X. E. Verykios, and R. Pitchai, “Support participation in chemistry of ethylene oxidation on silver catalysts,” *Appl. Catal.*, vol. 44, no. C, pp. 223–237, 1988.

[15] Voge Hervey H., “Problems in Heterogeneous Catalytic Oxidation,” vol. 76, pp. 242–253, 1968.

[16] P. A. Kilty and W. M. H. Sachtler, “the Mechanism of the Selective Oxidation of Ethylene To Ethylene,” *Catal. Rev. Sci. Eng.*, vol. 10, no. September 2012, pp. 1–16, 1974.

[17] A. Ayame, H. Kano, T. Kanazuka, and H. Baba, “Silver for Oxidation under of Ethylene over Catalyst Stationary State,” *Japan Pet. Inst.*, vol. 15, no. 2, 1973.

[18] P. J. Van Den Hoek, E. J. Baerends, and R. A. Van Santen, “Ethylene epoxidation on silver(110):

the role of subsurface oxygen," vol. 1981, no. 9, pp. 6469–6475, 1989.

[19] Z. Qu, M. Cheng, W. Huang, and X. Bao, "Formation of subsurface oxygen species and its high activity toward CO oxidation over silver catalysts," vol. 229, pp. 446–458, 2005.

[20] J. Greeley and M. Mavrikakis, "On the Role of Subsurface Oxygen and Ethylenedioxy in Ethylene Epoxidation on Silver," pp. 7992–7999, 2007.

[21] Y. Xu, J. Greeley, M. Mavrikakis, and W. Madison, "Effect of Subsurface Oxygen on the Reactivity of the Ag (111) Surface," no. 111, pp. 12823–12827, 2005.

[22] C. Backx, C. P. M. De Groot, and P. Biloen, "Adsorption of oxygen on Ag(110) studied by high resolution ELS and TPD," *Surf. Sci.*, vol. 104, no. 1, pp. 300–317, 1981.

[23] C. T. Campbell and M. T. Paffett, "The interactions of O2, CO and CO2 with Ag(110)," *Surf. Sci.*, vol. 143, no. 2–3, pp. 517–535, 1984.

[24] R. A. Van Santen and C. P. M. de Groot, "The Mechanism of Ethylene Epoxidation," vol. 539, pp. 530–539, 1986.

[25] T. C. R. Rocha, M. Hävecker, A. Knop-gericke, and R. Schlögl, "Promoters in heterogeneous catalysis : The role of Cl on ethylene epoxidation over Ag," *J. Catal.*, vol. 312, pp. 12–16, 2014.

[26] T. E. Jones, R. Wyrwich, S. Böcklein, E. A. Carbonio, M. T. Greiner, A. Y. Klyushin, W. Moritz, A. Locatelli, T. O. Menteş, M. A. Niño, A. Knop-Gericke, R. Schlögl, S. Günther, J. Wintterlin, and S. Piccinin, "The Selective Species in Ethylene Epoxidation on Silver," *ACS Catal.*, pp. 3844–3852, 2018.

[27] R. A. Van Santen and H. P. C. E. Kuipers, "The mechanism of ethylene epoxidation," *… Rev. …*, vol. 23, pp. 127–149, 1981.

[28] Boehning, Mross, Schwarzmann, Becker, Plueckhan, and Renner, "Silver catalyst and process for its preparation," 4829043, 1989.

[29] Boxhoorn and Klazinga, "Silver catalyst and process for its preparation," 4829044, 1989.

[30] D. Jingfa, Y. Jun, Z. Shi, and Y. Xiaohong, "Promoting effects of Re and Cs on silver catalyst in ethylene epoxidation," *J. Catal.*, vol. 138, no. 1, pp. 395–399, 1992.

[31] E. A. R. E. Hermans, "Master thesis Caesium and Chlorine promotion in the Silver particle size dependency and of the ethylene epoxidation by," Eindhoven Technical University, 2018.

[32] C. T. Campbell and B. E. Koel, "Chlorine promotion of selective ethylene oxidation over Ag(110): Kinetics and mechanism," *J. Catal.*, vol. 92, no. 2, pp. 272–283, 1985.

[33] C. T. Campbell and M. T. Paffett, "The role of chlorine promoters in catalytic ethylene epoxidation over the Ag(110) surface," *Appl. Surf. Sci.*, vol. 19, no. 1–4, pp. 28–42, 1984.

[34] S. N. Goncharova, E. A. Paukshtis, and B. S. Bal'zhinimaev, "Size effects in ethylene oxidation on silver catalysts. Influence of support and Cs promoter," *Appl. Catal. A, Gen.*, vol. 126, no. 1, pp. 67–84, 1995.

[35] V. I. Bukhtiyarov, I. P. Prosvirin, R. I. Kvon, S. N. Goncharova, and B. S. Bal'zhinimaev, "XPS study of the size effect in ethene epoxidation on supported silver catalysts," *J. Chem. Soc. - Faraday Trans.*, vol. 93, no. 13, pp. 2323–2329, 1997.

[36] T. W. Hansen, A. T. Delariva, S. R. Challa, and A. K. Datye, “Sintering of catalytic nanoparticles: Particle migration or ostwald ripening?,” *Acc. Chem. Res.*, vol. 46, no. 8, pp. 1720–1730, 2013.

[37] S. Amin, “Bimetallic Cu-Ag and Au-Ag catalyst for ethylene epoxidation reaction,” Eindhoven Technical University, 2018.

[38] S.-G. NorPro, “Norpro catalyst carriers.” [Online]. Available: https://www.norpro.saint-gobain.com/sites/imdf.norpro.com/files/sgnorpro-catalyst-carriers-typprop-nomenclature_0.pdf. [Accessed: 25-Jun-2018].

[39] J. T. Jankowiak and M. A. Barteau, “Ethylene epoxidation over silver and copper-silver bimetallic catalysts: I. Kinetics and selectivity,” *J. Catal.*, vol. 236, no. 2, pp. 366–378, 2005.

[40] G. Ertl, H. Knözinger, F. Schüth, J. Weitkamp, J. A. Dumesic, G. W. Huber, and M. Boudart, *, Chapter 11.3.4.1*, vol. 1. 2008.

[41] W. Diao, C. D. Digiulio, M. T. Schaal, S. Ma, and J. R. Monnier, “An investigation on the role of Re as a promoter in Ag-Cs-Re/α-Al2O3 high-selectivity, ethylene epoxidation catalysts,” *J. Catal.*, vol. 322, pp. 14–23, 2015.

[42] G. Audi and A. H. Wapstra, “Table of Isotopic Masses and Natural Abundances,” *Nucl. Phys. A*, vol. 565, pp. 1–65, 1993.

[43] A. Michaelides, M. L. Bocquet, P. Sautet, A. Alavi, and D. A. King, “Structures and thermodynamic phase transitions for oxygen and silver oxide phases on Ag{1 1 1},” *Chem. Phys. Lett.*, vol. 367, no. 3–4, pp. 344–350, 2003.

[44] H. J. Fan, U. Gösele, and M. Zacharias, “Formation of nanotubes and hollow nanoparticles based on kirkendall and diffusion processes: A review,” *Small*, vol. 3, no. 10, pp. 1660–1671, 2007.

Appendix A. Detailed description Matlab script

This script uses the following files: “Main16.n”,”Baseline.m”,”IntergratePeak.m” and “FitMS.m”. These files can be found attached with this report. Extra comments are present in the code.

First some general infrastructure is setup in “Main16”. The data is loaded in and a manual value PHIL is entered by the user. This stands for the time between pulses. The individual mass data is divided by the helium signal to account for fluctuations in pressure during the experiment.

In “Baseline” a few operations are carried out. First the moving average is calculated to more easily find peaks in the data. Then multiple methods are used to find the different peaks. Which method is used depends on the type of behavior the data shows (if data has a very inconsistent baseline a less accurate method needs to be used). But in general method 4 is used which will be explained here.

In this method a domain is chosen in the middle of the data. This has the width corresponding to the time setting defined earlier. This guarantees that there is at least one maximum and one minimum in the domain. The difference in height for these two points is calculated and this gives us a rough estimate for the average height that a peak of that signal will have. This value is then used as a criterion in the “findpeaks” function to find all peaks.

To create a baseline we take a peak position and move backwards over the x-axis until the difference in y-value is such that it can be considered static. This point will lie at the left bound base of each peak. This point is saved to be a baseline point. For the last point an alternative strategy is used. Here we take the two points before last. Calculate the distance between them and assume that the last baseline point will be the same distance further. These points are interpolated and then subtracted from the real data as baseline.

“IntergratedPeak” is used to integrate the area below each peak. The trapezoidal rule is used to calculate the area between the previously mentioned original baseline points.

Appendix B. Measuring of particles

For most particle size measurements it is quite straight forward on how to measure them. However for wetting particles this becomes more difficult. An example of this is shown in Figure 42. Here two wetting particles can be seen in the second transition of 60 hours of VC reaction. There are two ways of measuring marked, yellow and blue. In the report the blue method was used. However the yellow method would be more realistic to measure as particles, as these areas are assumed to be thicker and more particle-like. The lighter areas are assumed to be flatter disc like areas. Therefore for a more thorough analysis, both these values would have to be measured. Yellow could be added to the particle size distribution and blue could be used as a separate value to indicate the size of wetting areas. By using another method the number of particles also changes. Every one particle initially exhibiting wetting could form 1, 2 or even more new particles and might create 1 or in some 2 flat areas.

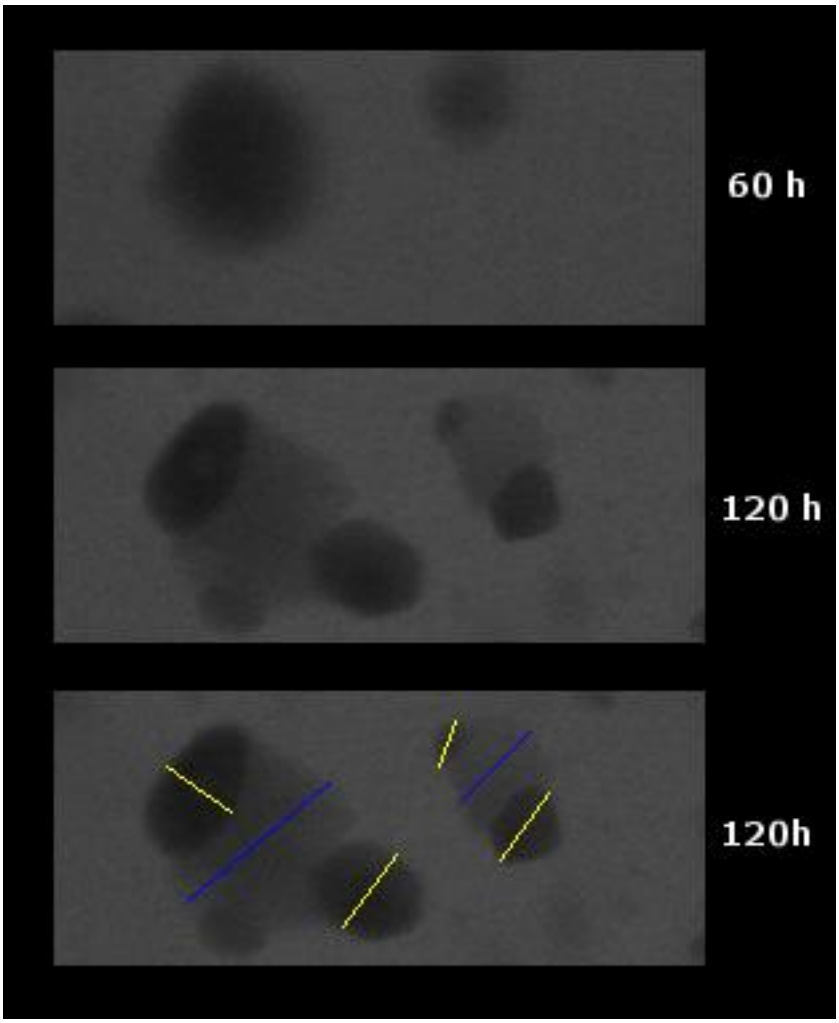

Figure 42. Example of two ways to measure particle size for a wetting particle.